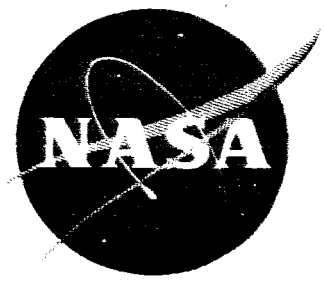

Quarterly Progress Report No. 1

INVESTIGATION OF ELECTRON EMISSION CHARACTERISTICS OF LOW WORK FUNCTION SURFACES

by

L. W. Swanson
L. C. Crouser

Prepared for

Lewis Research Center
NASA, Cleveland 35, Ohio

CONTRACT NASw-1082

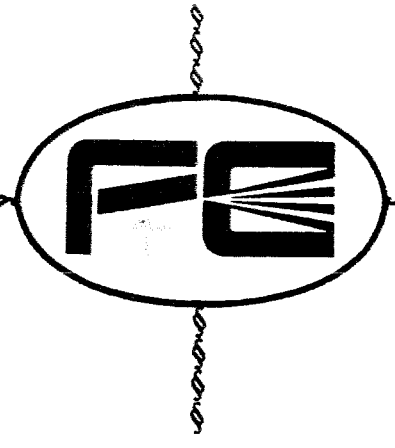

Field Emission Corporation

McMinnville, Oregon

Quarterly Progress Report No. 1
for the Period
28 September 1964 to 27 December 1964

INVESTIGATION OF ELECTRON EMISSION CHARACTERISTICS OF LOW WORK FUNCTION SURFACES

by

L. W. Swanson
L. C. Crouser

Prepared for

Lewis Research Center
NASA, Cleveland 35, Ohio

27 January 1965

CONTRACT NASw-1082

FIELD EMISSION CORPORATION
Melrose Avenue at Linke Street
McMinnville, Oregon 97128

TABLE OF CONTENTS

	Page
PURPOSE	1
ABSTRACT	2
PROGRESS TO DATE	3
INTRODUCTION	4
The Advantage of Low Work Function Surfaces	5
Recent Work on Low Voltage Field Emission	9
EMISSION HEATING AND COOLING	14
Theory	16
Experimental Techniques	21
Results and Discussions	28
Summary	47
TEMPERATURE DEPENDENCE OF WORK FUNCTION	48
ENERGY DISTRIBUTION MEASUREMENTS	52
FUTURE WORK	53
REFERENCES	54

LIST OF ILLUSTRATIONS

Figure 1.	Field emission patterns of a (100) oriented tungsten emitter showing the alteration of the emission distribution before (photo a) and after (photo b) co-deposition of zirconium and oxygen.	10
Figure 2	Field emission work function as a function of average cesium atom density for clean tungsten and for two degrees of underlying oxygen coverage.	12

		Page
Figure 3.	Field emission work function as a function of desorption temperature for cesium on the indicated substrates. The emitter was heated for 60 seconds at the indicated temperature prior to each work function determination.	13
Figure 4.	Potential energy diagram and total energy distribution for field or T-F emitted electrons.	17
Figure 5.	Diagram of tip assembly used in tube for studying emission heating and cooling.	23
Figure 6.	Diagram showing tip assembly, associated filaments and electrodes for quantitative study of emission heating and cooling.	24
Figure 7.	Plot of experimentally determined conversion factor (for converting ΔR changes to H) as a function of emitter temperature.	26
Figure 8.	Experimentally determined power exchange H at the emitter as a function of field emitted current I_e at the indicated temperatures and work function.	31
Figure 9.	Experimentally determined power exchange H at the emitter as a function of field emitted current I_e at the indicated temperatures and work function.	32
Figure 10.	Experimentally determined power exchange H at the emitter as a function of field emitted current I_e at the indicated temperatures and work function.	33
Figure 11.	Experimentally determined power exchange H at the emitter as a function of field emitted current I_e at the indicated temperatures and work function.	34
Figure 12.	Experimentally determined power exchange H at the emitter as a function of field emitted current I_e at the indicated temperatures and work function.	35
Figure 13.	Experimentally determined power exchange H at a tungsten emitter coated with zirconium-oxygen as a function of field emission current I_e. Negative values of H indicate emission cooling.	37

Page

Figure 14. Experimentally determined energy exchange per electron A with the tungsten lattice as a function of applied electric field F at the indicated temperatures and work functions. Also shown are the corresponding theoretical curves calculated according to equation (12). 39

Figure 15. Experimentally determined energy exchange per electron A with the tungsten lattice as a function of applied electric field F at the indicated temperatures and work functions. Also shown are the corresponding theoretical curves calculated according to equation (12). 40

Figure 16. Experimentally determined energy exchange per electron A with the tungsten lattice as a function of applied electric field F at the indicated temperatures and work functions. Also shown are the corresponding theoretical curves calculated according to equation (12). 41

Figure 17. Experimentally determined energy exchange per electron A with the tungsten lattice as a function of applied electric field F at the indicated temperatures and work functions. Also shown are the corresponding theoretical curves calculated according to equation (12). 42

Figure 18. Experimentally determined energy exchange per electron A with the tungsten lattice as a function of applied electric field F at the indicated temperatures and work functions. Also shown are the corresponding theoretical curves calculated according to equation (12). 43

Figure 19. Experimentally determined energy exchange per electron A with the tungsten lattice as a function of applied electric field F at the indicated temperatures and work functions for a zirconium-oxygen coated emitter. Negative values of A indicate emission cooling. Calculated curves were determined according to equation (12) and assuming $p=1.685\ p_{calc.}$ 44

Figure 20. Experimentally determined inversion temperatures for a zirconium-oxygen coated tungsten emitter (ϕ=2.67 ev) as a function of applied electric field. Dashed curve is calculated inversion temperature according to equation (13). 46

Page

Figure 21. Plot of work function change of a zirconium-oxygen coated tungsten emitter (as determined from slopes of Fowler-Nordheim plots) as a function of emitter temperature. 50

Figure 22. Fowler-Nordheim plots of a zirconium-oxygen coated tungsten emitter at two different values of emitter temperature. Curvature in curve (b) is due to increasing importance of T-F emission at high temperatures and low fields. 51

PURPOSE

The primary aims of this investigation are to obtain an improved fundamental understanding of (1) the phenomena governing the production of low work function surfaces, and (2) the factors affecting the quality and stability of electron emission characteristics of such surfaces. It is expected that the information generated from this investigation will be relevant to various kinds of electron emission (i.e., photo, thermionic and field emission), although the primary emphasis will be placed upon field electron emission. Accordingly, field emission techniques will be employed, at least initially, to obtain the objectives of this research.

The formation of low work function surfaces will be accomplished by (1) adsorption of appropriate electro-positive adsorbates, (2) co-adsorption of appropriate electro-positive and electro-negative adsorbates and (3) fabrication of emitters of low work function surfaces from various metalloid compounds. The various properties of these surfaces to be investigated in order to obtain a more fundamental understanding of them are the temperature dependency of the emission and work function, the various types of energy exchanges accompanying emission, the energy distribution of the emitted electrons, and various aspects of the surface kinetics of adsorbed layers such as binding energy, surface mobility and effect of external fields.

ABSTRACT

2133

Measurements of the energy exchange accompanying field emission have been performed on clean tungsten and zirconium-oxygen coated tungsten surfaces. The results obtained show the occurrence of both a heating and a cooling mechanism accompanying field emission depending on the exact value of the temperature, work function and applied electric field. In the case of Zr/O_2 coated tungsten surfaces with a work function of 2.6 ev, emission cooling occurred for temperatures above 450°K at an electric field of 23 Mv/cm; clean tungsten surfaces exhibiting a work function of 4.52 ev gave evidence of emission cooling for temperatures above 1090°K at an electric field of 48 Mv/cm. Although the general features of the existing theory of "Nottingham" emission heating and cooling were confirmed, certain discrepancies were noted between experiment and theory in regard to the amount of energy exchanged per electron and the value of the temperature boundary which separates emission heating and cooling.

A brief investigation of the variation of field emission with temperature for Zr/O_2 coated tungsten surfaces has been performed over the temperature range 300°K to 1100°K. An increase in the emission with temperature was observed and attributed both to a decrease in work function with increasing temperature and predicted increase due to thermal-enhanced field emission. A coefficient of work function change with temperature of approximately 10^{-3} ev/degree was found.

AUTHOR ↑

PROGRESS TO DATE

Progress is being made in four general areas of investigation of low work function surfaces obtained by co-adsorption. They are: (1) emission heating; (2) energy distribution; (3) surface kinetics; (4) work function change on single crystallographic planes. The investigation of the preceding phenomena involves different tube embodiments which have been constructed and are currently being used to obtain results. Prior to the commencement of this investigation, preliminary results were obtained in the areas of emission heating and various aspects of the co-adsorption of cesium and oxygen on tungsten and have been reported elsewhere[1-4].

During this quarter moderate progress has been made in the investigation of energy exchange mechanisms accompanying field emission over a wide range of temperatures (300 - 1100°K), work function (4.6 - 2.2 ev), total emitted current (0 - 500 μa) and applied electric fields (20 - 55 Mv/cm). The latter investigation was performed on both a clean tungsten emitter and an emitter contaminated with oxygen and/or zirconium in order to vary the work function.

An experimental tube was constructed for the purpose of measuring energy exchange phenomena at the tip of a field emitter. The sensitivity of this tube was such that energy exchange phenomena causing power inputs at the tip as low as 5 μw could be easily detected. Provisions for the admittance of various adsorbates on the emitter were also included.

Construction of a tube capable of measuring the total energy distribution of field emitted electrons from clean or coated tungsten surfaces has

been completed and preliminary measurements are currently underway. This tube is also provided with a means of magnetically deflecting the field emission beam so that energy distributions from various single crystallographic planes can be measured. It is expected that the results of this investigation will shed considerable light on some of the discrepancies observed between the experimentally obtained and theoretically expected results of the energy exchange processes during emission.

A conventional field electron microscope capable of admitting both cesium and/or oxygen onto a field emitter has been constructed and is currently undergoing tests. Experimental work functions as low as 1.1 ev have been observed for this system in previous work.[4]

In addition to the above described experimental tubes, a "probe tube" has also been constructed which allows measurement of single plane work functions of a field emitter with or without the presence of various adsorbates. This tube has been successfully evacuated and will be used primarily for investigating work function changes on various crystallographic planes of tungsten and other refractory metal emitters in the presence of various adsorbates which lower the work function. This tube can also be used to study field desorption from single crystallographic planes.

INTRODUCTION

Whereas the initial phase of this work is dedicated toward a greater fundamental understanding of the attainment and behavior of low work function

surfaces suitable for field emission cathodes, it is expected that these results will lead to the fulfillment of the overall practical objective of this work, namely to develop and make available to space technology electronic devices which derive special advantages from the use of field emission cathodes. Of the numerous advantages of field emission cathodes, perhaps the properties of interest to space applications are the relative insensitivity of field cathodes and, therefore, of their performance to radiation bombardment and to large variations in ambient temperature.

Smoothly rounded field emission cathodes made of pure tungsten have been available for some time; however, such cathodes which possess a fairly high work function normally require applied grid voltages of 1 kv for field emission at high current density levels, and it is therefore difficult to derive or modulate such cathodes by means of solid state devices. In order to meet such practical objectives it will be necessary to develop field emission cathodes which are capable of high density electron emission at grid voltages well below 1 kv, and whose emission density can be modulated from practical cut-off to a level of the order of 10^7 amps/cm^2 by means of applying grid signals of the order of 100 volts or even less.

THE ADVANTAGE OF LOW WORK FUNCTION SURFACES

There are basically two possible approaches which may be followed to achieve field emission at low voltages. Starting from the basic zero degree approximation field emission law:

$$J_{oF} = CF^2 \exp(-b\,\phi^{3/2}/F) \qquad (1)$$

Where J_{oF} is the emitted current density, F the applied field, ϕ the electron work function and b and C are constants, one obtains the following relationship between the field emitted current I and the applied grid voltage V:

$$I = AJ_{oF} = A' \beta^2 V^2 \exp(-b\phi^{3/2}/\beta V) \tag{2}$$

where A is the effective emitting area and $\beta = F/V$ is a geometrical factor defined as the ratio of the electric field F produced at the field emitter apex to the applied grid voltage V. For a typical needle-shaped field emission cathode with a smoothly rounded tip having a radius of curvature r at the apex, it can further be shown that the β factor is approximately equal to:

$$\beta = \frac{1}{r \log \frac{4R}{r}} \tag{3}$$

where R is the cathode to grid spacing.

In view of equations (2) and (3), it is readily seen that the grid voltage V which is required for a given emission density is roughly proportional to $r\phi^{3/2}$, so that V may be reduced either by using a sharper tip or by reducing the work function ϕ of the cathode. It is in practice difficult to reconcile effective cathode shaping and processing techniques with tip radii much less than 10^{-5} cm which corresponds to a minimum required grid voltage of the order of 1 kv for a clean tungsten emitter. Furthermore, it will be noted that use of a very small tip radius leads to a small emitting area, and therefore to a relatively low total emitted current for a given value of emission density.

An alternative approach to low voltage field emission is through a reduction of the electron work function ϕ of the emitting surface. Equations (1) and (2) show that, at least at emission density levels low enough that space charge effects are not pronounced (i.e., for $J=10^5$ amp/cm^2), a given total current will be emitted by a cathode of a given tip radius r at a grid voltage approximately proportional to the 3/2 power of the work function; for instance, the required grid voltage can be reduced by a factor of 8 by going from a clean tungsten (for which $\phi=4.52$ ev) to an appropriate coating of cesium and oxygen on a tungsten substrate (for which $\phi=1.15$ ev). Even at very high emission density levels where space charge effects become pronounced, the use of an emitting surface with low work function still yields a very substantial reduction in the grid voltage required for a given cathode current.

In view of the preceding discussion, the low work function approach appears preferable. Until recently, this approach was discouraged by a lack of pure materials having a sufficiently low work function and possessing other characteristics required of satisfactory field cathode materials, and by the lack of surface coatings capable of sufficient reduction in work function (e.g., down to $\phi=2.0$ ev) and still having sufficient stability to provide a practical cathode surface. However, recent work has indicated that by successful deposition of appropriate amounts of oxygen and of cesium on a tungsten substrate, it was possible to achieve a very low work function. In addition, preliminary investigations have shown a reasonable thermal stability for this coating.

Another important advantage of the low work function coating is that it results in modification of the initial distribution of the field emitted electrons in a direction which both reduces the energy spread and increases the average energy of the emitted electrons - the basic reason for this will be discussed more fully in a later section. The mean spread in initial energy of field emitted electrons, and therefore the beam noise, are in fact approximately proportional to the work function (for a given emission density); thus, at a typical emission density of 10^7 amp/cm^2, the minimum spread in energy for a clean tungsten cathode is approximately 0.28 ev (corresponding to an equivalent beam noise temperature of approximately 3200°K) whereas the mean spread for the Cs/OW cathode is predicted to be only 0.07 ev (corresponding to a much cooler beam with a noise temperature of approximately 800°K).

The increase in the average energy of emitted electrons which also accompanies a reduction in the work function is equally significant because it leads to a reduction in the amount of heat transferred to the cathode by the emitted electrons for a given emission density. For instance, steady state field emission at a current density of 10^7 amp/cm^2 leads to an increase in tip temperature of approximately 1200°K for a pure tungsten cathode, whereas it should increase the tip temperature by only 150°K in the case of a Cs/OW cathode. This reduction in tip temperature may be more than sufficient to off-set the reduction in maximum permissible tip temperature which results from use of the coating. Indeed, this has been demonstrated experimentally in the case of Zr/OW and Cs/OW coated cathodes.

RECENT WORK ON LOW VOLTAGE FIELD EMISSION

Recent studies have been concerned with coatings of zirconium and cesium in the presence of oxygen on a tungsten substrate. Zirconium-oxygen coated tungsten field cathodes have undergone preliminary study under DOD support[3]. Work function reduction which it allows (2.6 ev for the coated surface as opposed to 4.52 ev for pure tungsten) is not as large as that which can be achieved with cesium-oxygen coatings, but does have certain effects on the emission distribution as shown in Figure 1, which makes it of interest for possible cathode applications.

Extensive basic studies of the physical and electrical properties of coatings of cesium on clean refractory metals, including tungsten, have been performed at this laboratory for the past three years under NASA support,[4, 5] in a supporting research program related to ion propulsion system development. Since cesium atoms have exceptionally low ionization potential and high polarizability, cesium coating on a substrate metal of reasonably high work function leads to a very large reduction in the electron work function of the surface. This has been confirmed experimentally by a number of investigators, and the minimum work function for cesium on clean tungsten (corresponding to a degree of cesium coverage approximately 2/3 of a monolayer) is approximately 1.6 ev. However, it is found that this relatively large degree of coverage can be maintained on the clean tungsten substrate only at temperatures below 300°K, which means that such a coating would provide a time stable electron source only if the cathode were refrigerated to very low temperatures; even then, the permissible emission density

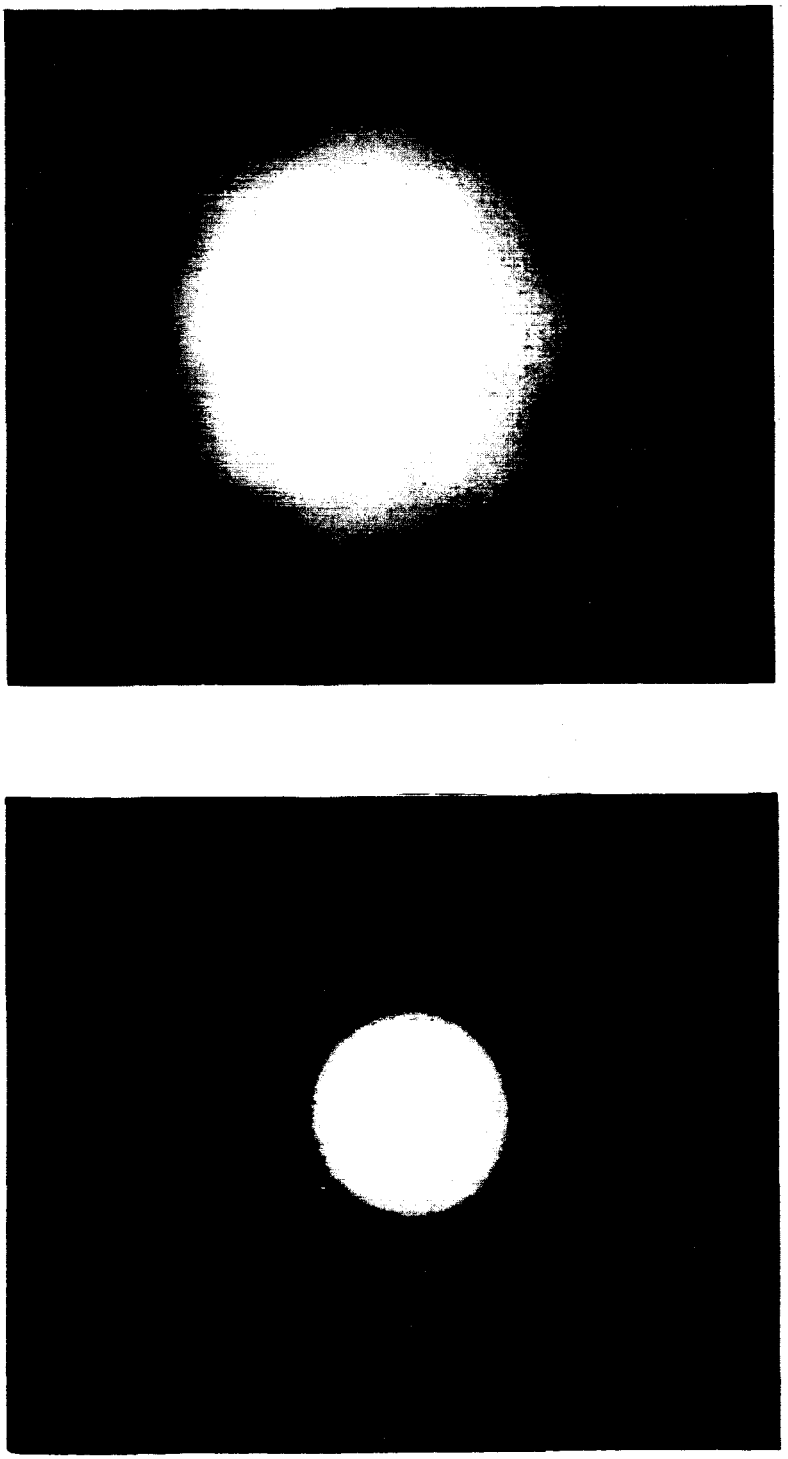

Figure 1. Field emission patterns of a (100) oriented tungsten emitter showing the alteration of the emission distribution before (photo a) and after (photo b) co-deposition of zirconium and oxygen.

would be severely limited by the inadequate temperature stability of the coating, since the field emission process inherently produces some heating of the tip. However, it has been found that the presence of oxygen can greatly stabilize the cesium coating with respect to surface mobility and thermal desorption. This can be shown by referring to Figures 2 and 3 which show the amount of cesium necessary to obtain a given work function for various underlying amounts of oxygen and the stability of a cesium coating with respect to thermal desorption also for various underlying amounts of oxygen, respectively. The results of these studies show that oxygen, particularly at a fairly high degree of coverage, has two effects on the Cs/W system which are very favorable in terms of the possible use of that system as a practical cathode surface: First, even though oxygen raises the tungsten work function in the absence of cesium, Figure 2 shows that the lowering of the work function with increased cesium coverage is much more rapid in the presence of oxygen, so that a still lower work function minimum of approximately 1.13 ev can be achieved, corresponding to a lesser amount of cesium than was necessary in the absence of oxygen; Second, as shown in Figure 3, the addition of oxygen greatly increases the temperature stability of the cesium coating, so that the optimum cesium coating corresponding to a minimum work function is now stable up to a temperature of approximately 515°K, as opposed to 330°K in the absence of oxygen.

The preliminary results obtained thus far demonstrate the feasibility of forming of field emitters with very low work function surfaces and thereby lend encouragement to the possible utilization of such cathodes for special

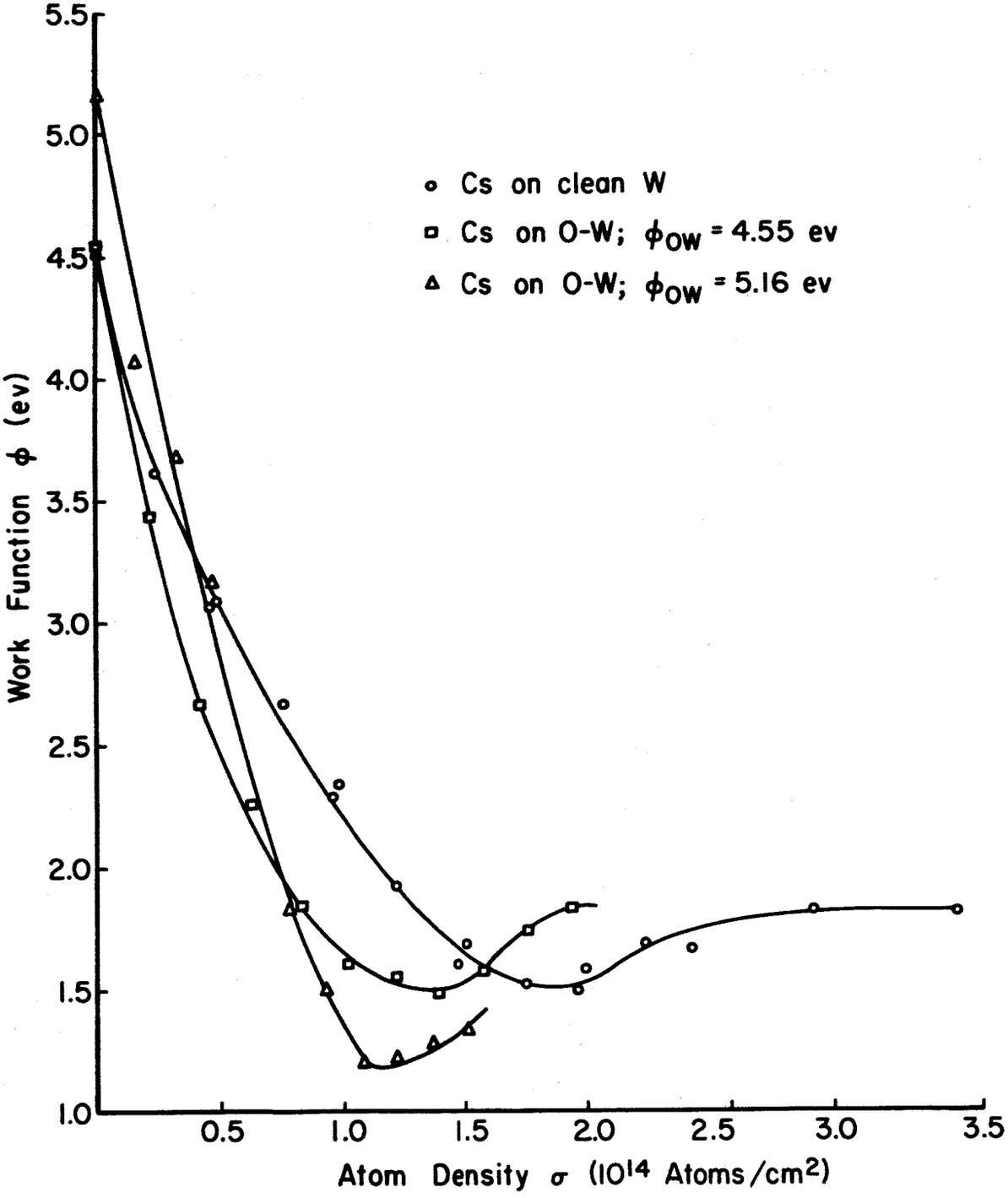

Figure 2. Field emission work function as a function of average cesium atom density for clean tungsten and for two degrees of underlying oxygen coverage.

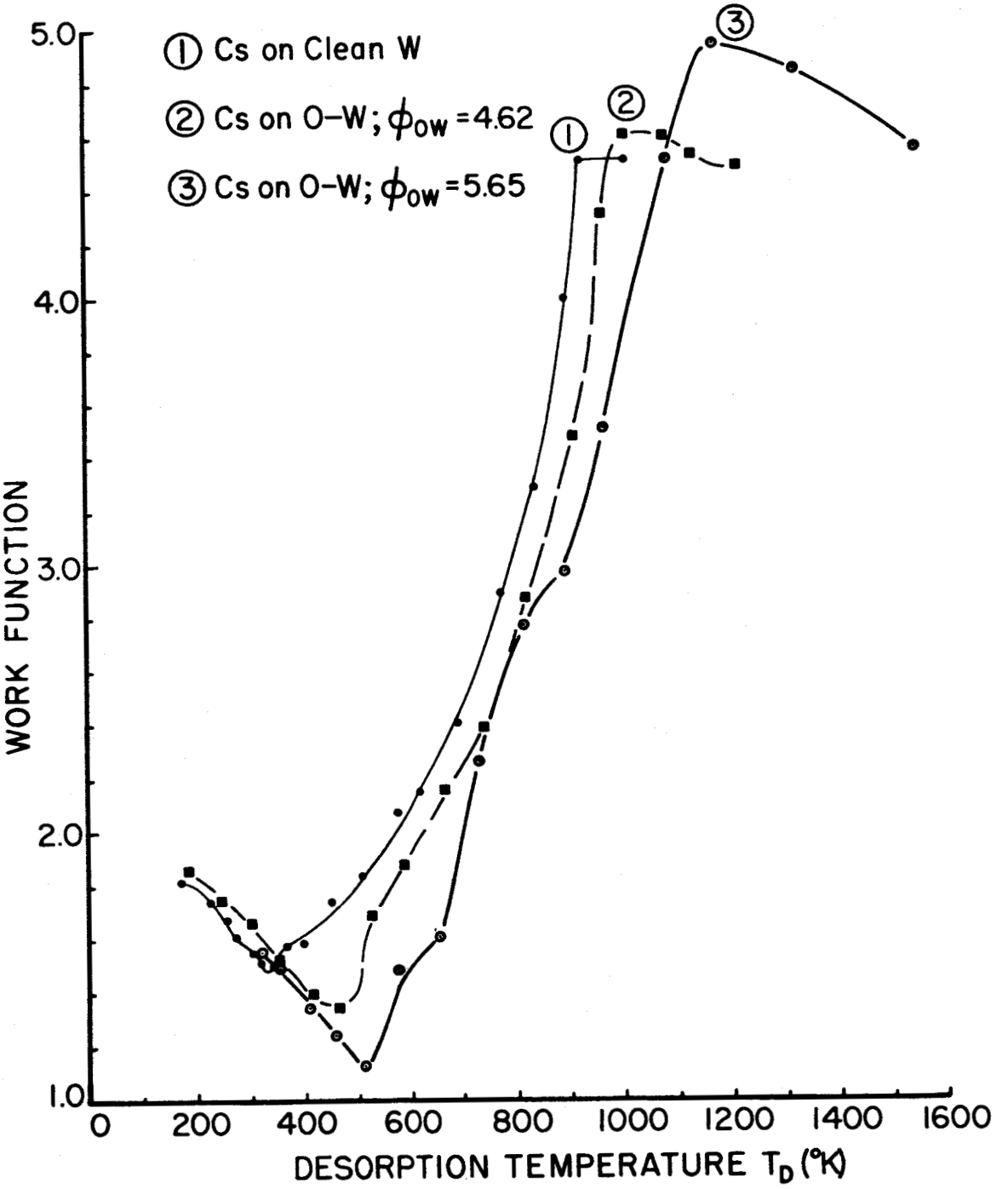

Figure 3. Field emission work function as a function of desorption temperature for cesium on the indicated substrates. The emitter was heated for 60 seconds at the indicated temperature prior to each work function determination.

electronic applications. It is apparent, however, that further fundamental knowledge of these systems is needed before further improvements in the stability and reliability of such surfaces can be obtained. Therefore, the initial effort in this work will be directed toward the latter goal, with the expectation that knowledge so generated will also be of value to other applications of low work function surfaces such as thermionic converters.

EMISSION HEATING AND COOLING

Electron emission is accompanied by energy exchanges between the conduction electrons and lattice, which become particularly important at very high emission densities feasible with field and T-F emission cathodes. Their study is of basic interest as it provides a complimentary check, through a direct measurement of the average energy of emitted electrons, of the theory of field and T-F emission; it is also of practical importance because these energy exchanges control the cathode tip temperature and set an upper limit on the feasible emission density. The work reported herein is an attempt to confirm the theoretically predicted temperature dependence of the energy exchange and its reversal (from cathode heating to cooling) at high temperatures.

There are two main emission induced energy exchange phenomena. The familiar resistive or Joule heating effect was first studied in the case of field emission by Dyke, et al[6], and Dolan, Dyke and Trolan[7]. In the usual case where resistivity increases rapidly with temperature, resistive heating by itself leads to an inherently unstable situation at high emission

densities. Since stable high density emission is observed[8], there must exist another factor having a strong and stabilizing influence on the cathode-tip temperature.

Such a stabilizing factor is provided by the energy exchange resulting from the difference between the average energy of the emitted electrons, $\bar{E}$ and that of the replacement electrons supplied from the Fermi sea, $\bar{E}'$. In the case of thermionic emission this phenomenon, discussed by Richardson[9] and later by Nottingham[10], is well known and produces cooling of the cathode by an average amount $\phi+2kT$ per emitted electron. The corresponding effect in field and T-F emission was first discussed by Fleming and Henderson[11], who were unable to detect it experimentally and has been a subject of controversy[10,11], with respect to the correct value of $\bar{E}'$ and hence the direction of the effect (cathode cooling occurs when $\bar{E}>\bar{E}'$, and heating when $\bar{E}<\bar{E}'$). Data generated thus far tends to support the view of Nottingham, who took $\bar{E}'$ to be the Fermi energy E_f and, on that basis, predicted heating of the cathode in the case of field emission. Thus, replacement electrons assumed to have the Fermi energy and their corresponding energy exchange will be referred to as the "Nottingham effect".

The combined effect of resistive and Nottingham phenomena has been treated in the special case of tungsten field emitters initially at room temperature[12]; this work was later extended to other work functions and confirmed experimentally[13]. Levine[14] gave a theoretical analysis of a similar problem. Drechsler[15,16] has recently reported both departure and agreement with theoretical predictions for the temperature dependence of

the Nottingham effect and for the value of the inversion temperature for tungsten.

THEORY

In order to more clearly understand the energy exchange phenomena accompanying field emission, it is instructive to derive expressions for the total energy distribution $P(E)dE$ and the average energy for field emitted electrons. The situation is depicted in Figure 4 which gives a one-dimensional potential plot of the surface of a metal (free electron model assumed) with a work function ϕ and externally applied electric field F. At $T=0^{o}K$ all electron levels of the metal above the Fermi level are empty and all emitted electrons must necessarily originate from energies below the Fermi level. Following the original derivation of the total energy distribution by Young and Mueller[17], we can formulate an expression for the number of electrons whose total energy lies within the range E to E+dE by a product of a supply function $N(E_x, E)$ and a barrier penetration coefficient $D(E_x)$ in the following fashion:

$$P(E)\,dE = \int_{E}^{-V_o} N(E_x, E)\, D(E_x)\, dE_x dE \qquad (4)$$

The expression for the supply function which is the number of electrons with energy within the range E to E+dE whose x part of the energy lies in the range of E_x to E_x+dE_x is given by:

$$N(E_x, E)dE_x dE = \frac{-4\pi\, m\, dE_x dE}{h^3\,(e^{\epsilon/kT}+1)} \qquad (5)$$

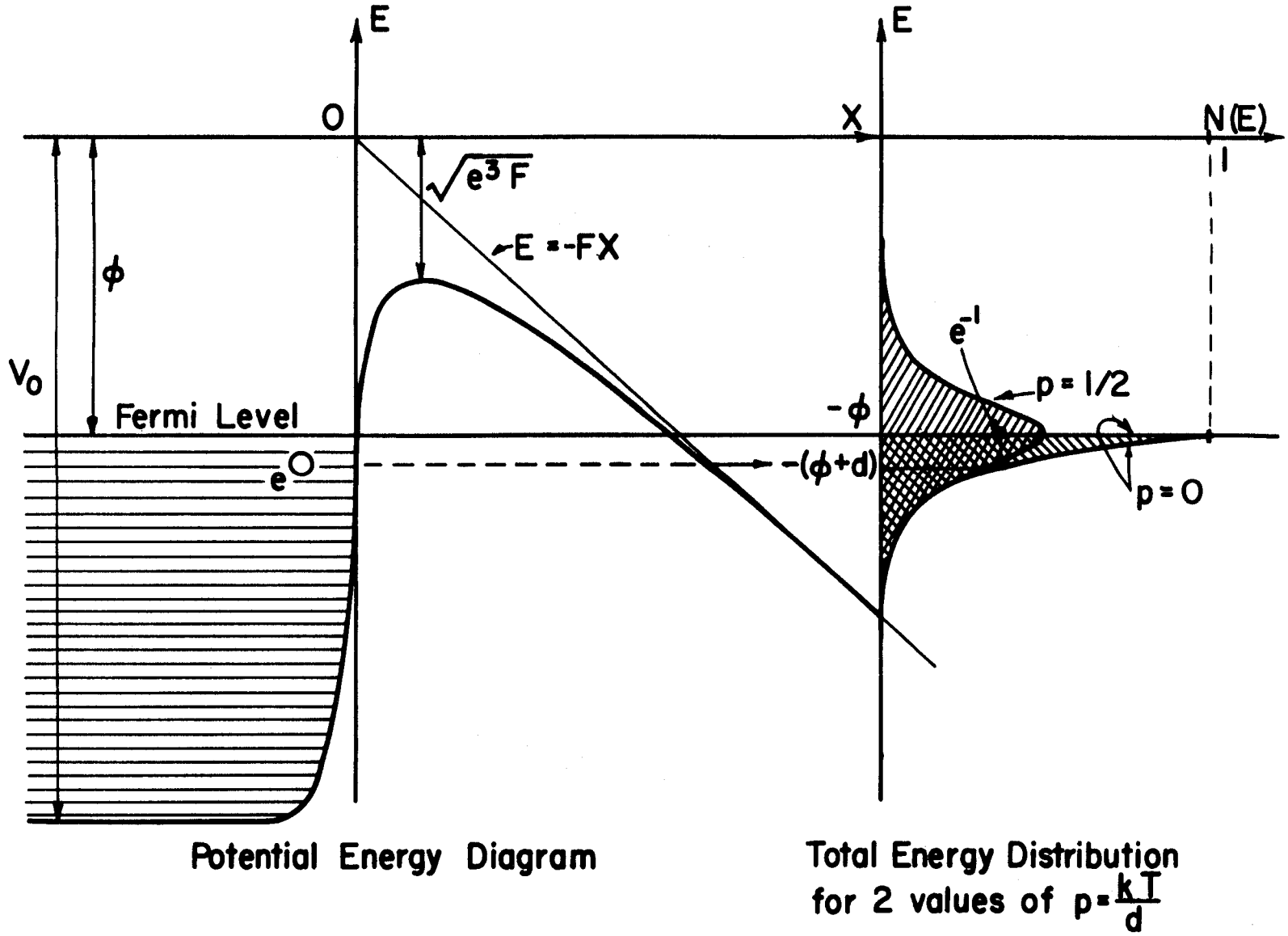

Figure 4. Potential energy diagram and total energy distribution for field or T-F emitted electrons.

where $\epsilon = E - E_f$ is the energy of the electron relative to the Fermi level. An approximate expression for the transmission coefficient valid in the range $E_x \cong E_f$ is:

$$D(E_x) = e^{-c+(E_x+E_f)/d} \tag{6}$$

where:

$$c = \frac{4}{3} \frac{(2m\phi^3)^{1/2}}{\hbar eF} \quad v(y) \tag{7}$$

$$d = \frac{\hbar eF}{2(2m\phi)^{1/2} t(y)} \tag{8}$$

and t(y) and v(y) are tabulated slowly varying functions of ϕ and F. When $E_x = -V_o$ the integrand of equation (4) is essentially zero and the integration is facilitated by setting the limit $-V_o$ equal to $-\infty$; performing the integration leads to the following expression for the total energy distribution of field emitted electrons relative to the Fermi level:

$$P(\epsilon)\, d\epsilon = \frac{4\pi m\, d\, e^{-c}\, e^{\epsilon/d}}{h^3 (d^{\epsilon/kT} + 1)}\, d\epsilon \tag{9}$$

The above equation shows that the total energy distribution function is the product of a field and work function dependent transmission coefficient and the Fermi-Dirac distribution function. Multiplying equation (9) by the electronic charge and integrating over the limits $-\infty$ to ∞ will yield an expression for the current density of the field emitted electrons. This integration can be accomplished by defining a dimensionalless parameter p=kT/d which

leads to an expression for the current density J_{TF} of T-F emission of the following form:

$$J_{TF} = \frac{\pi p}{\sin \pi p} \frac{F^2 e^{-c}}{8 \pi h \phi t^2(y)} = \frac{\pi p}{\sin \pi p} J_{oF} \qquad (10)$$

which is valid only in the range $0 \leq p \geq 2/3$. For small values of p (i.e., low temperatures or high fields) $\pi p/\sin \pi p \tilde{=} 1$ and one obtains the $0^{o}K$ approximation of the Fowler-Nordheim formula given in equation (1).

With an analytical expression for the total energy distribution it is possible to obtain an expression for the average energy $\bar{\epsilon}$ by performing the following integration:

$$\bar{\epsilon} = \frac{\int_{-\infty}^{\infty} \epsilon P(\epsilon) d\epsilon}{\int_{-\infty}^{\infty} P(\epsilon) d\epsilon} = -d f(p) \qquad (11)$$

Levine[14] has shown that the function $f(p) - \pi p/\tan \pi p$ so that equation (11) may be written in an alternative form:

$$\bar{\epsilon} = -\pi kT \cot \pi p \qquad (12)$$

which is also valid over the range $0 \leq p \geq 2/3$. The form of equation (12) predicts a dependency of $\bar{\epsilon}$ on T, F and ϕ; it is also apparent that $\bar{\epsilon} = 0$ when $p = 1/2$. Physically, this means that electrons are emitted from energy levels both above and below the Fermi level with equal probability when $p = 1/2$; or, alternatively, the energy distribution predicted by equation (9) is symmetrical

about the Fermi level. In fact, it can be shown that the shape of the energy distribution curve of equation (9) depends only on the dimensionalless parameter p.

The significance of the condition p=1/2 is that, if the holes left in the metal by the emitting electrons are filled by electrons possessing energy at or very near the Fermi level, then there will be no net energy exchange during emission. Whether electron holes are in fact filled by electrons with the Fermi energy, and furthermore, whether this process occurs near the emitting surface, has been the subject of controversy in the past. Both experimental results and theoretical considerations of the mean free path for electron-electron and electron-phonon interactions for electrons (or holes) near the Fermi energy suggest the occurrence of such energy exchange processes within the dimensions of an emitter tip, which is the order of 10^{-5} cm. Perhaps the primary question yet to be answered is the exact distribution of levels (i.e., the Fermi level or levels slightly above or below) from which the electrons originate which ultimately fill the empty holes for various lattice temperatures.

From the preceding considerations one can define an inversion temperature T^* for which the energy distribution is symmetrical about the Fermi level:

$$T^* = \frac{d}{2k} = \frac{5.67 \times 10^{-5} F}{t(y)\, \phi^{1/2}} \quad (^{\circ}K) \tag{13}$$

for F in v/cm and ϕ in ev. Thus, the inversion temperature is a function of F and ϕ and can be examined experimentally and compared with energy distributions at T^* for experimental self-consistency.

EXPERIMENTAL TECHNIQUES

The main difficulty in measuring energy-exchange phenomena in field and T-F emission is the usually strong localization of these phenomena and of the associated temperature changes; this localization results from the cathode geometry (very sharp needle with a conical shank and tip radius well below 1 μ) with which controlled field emission is most reliably obtained. A determination of both magnitude and location of the energy transfer requires measurement of the temperature at the emitting area itself, which is of the order of 10^{-9} cm^2. For this purpose, adsorbed layers whose coverage, and hence work function, vary with temperature can be used to sense the local tip temperature. Measurements of this type have been performed[13] and conclusively establish the existence of emission heating and cooling domains and, within the limited accuracy feasible, confirm the magnitude of the effect and indicate the transfer of energy to occur within a few tip radii of the cathode tip. However, the complex experimental conditions (pulsed emission, large field and temperature gradients near the tip, etc.) limit the accuracy of the results and, in the work presently reported, a more precise method has been used to measure magnitude (but not location) of the energy exchange and inversion temperature.

The method used here is a refinement of that of Drechsler[15, 16], who obtained field and T-F emission from random protrusions on the surface of very thin wires. The principle is to give the emitter-support filament sufficient thermal impedance that the small heat input resulting from T-F

emission at relatively low current levels may be detected sensitively through the associated change in temperature and resistance of the filament. Reliance on emission from several random protrusions of unknown number, geometry and location creates uncertainties in interpretation of the data which are avoided here by confining emission to a single field-emission needle (whose precise geometry has been determined in an electron microscope) mounted at the center of a smooth support wire 1" long and approximately 1.1 mil in diameter. The diagram of the tip assembly shown in Figure 5 consists of two 40-mil filaments supporting the emitter support wire to which two 0.5-mil potential leads are spot welded for sampling resistance changes across a 200 mil portion of the emitter support filament. The central 1.1 mil diameter lead carries the emission current in order to eliminate any IR drops on the emitter support filament due to the emission current itself. The temperatures of the emitter and emitter support filament are controlled by adjusting a DC heating current passed through the filament; the temperature is measured by the resistance change ΔR of the 200 mil section of the emitter support filament. The thermal impedance of the structure is high enough that emission-induced power inputs can be measured with an accuracy of 5 μw, permitting reliable measurements at low current levels where resistive heating is calculable and small and where, therefore, the Nottingham effect strongly predominates and is more effectively studied.

The present embodiment also permits correct calibration of ΔR, due to emission heating, in terms of input power at the tip: For this purpose, the tip is bombarded by a very fine 30 by 5 mil electron sheet beam generated by an auxiliary filament D of Figure 6 and focused by an 800 gauss magnetic

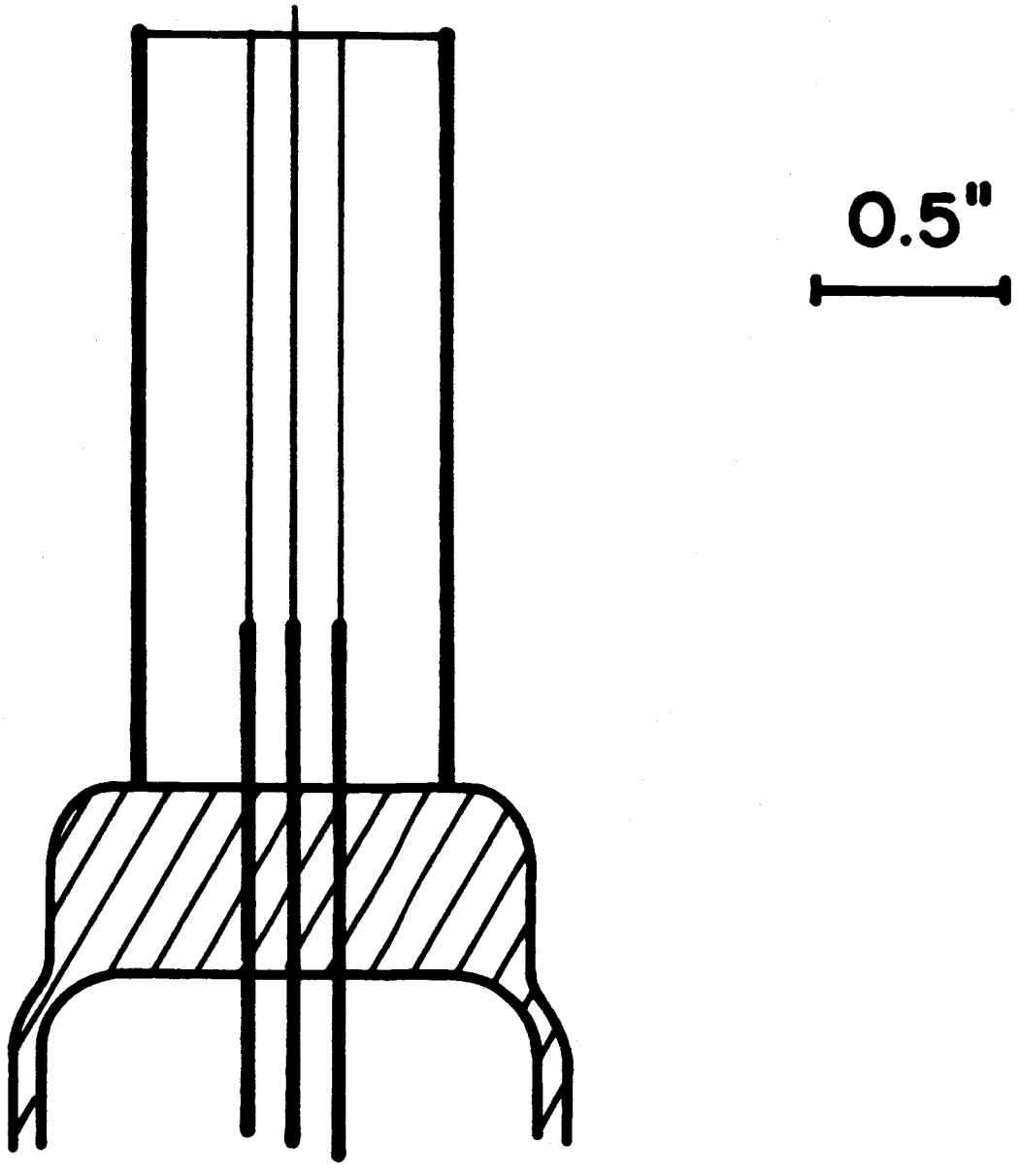

Figure 5. Diagram of tip assembly used in tube for studying emission heating and cooling.

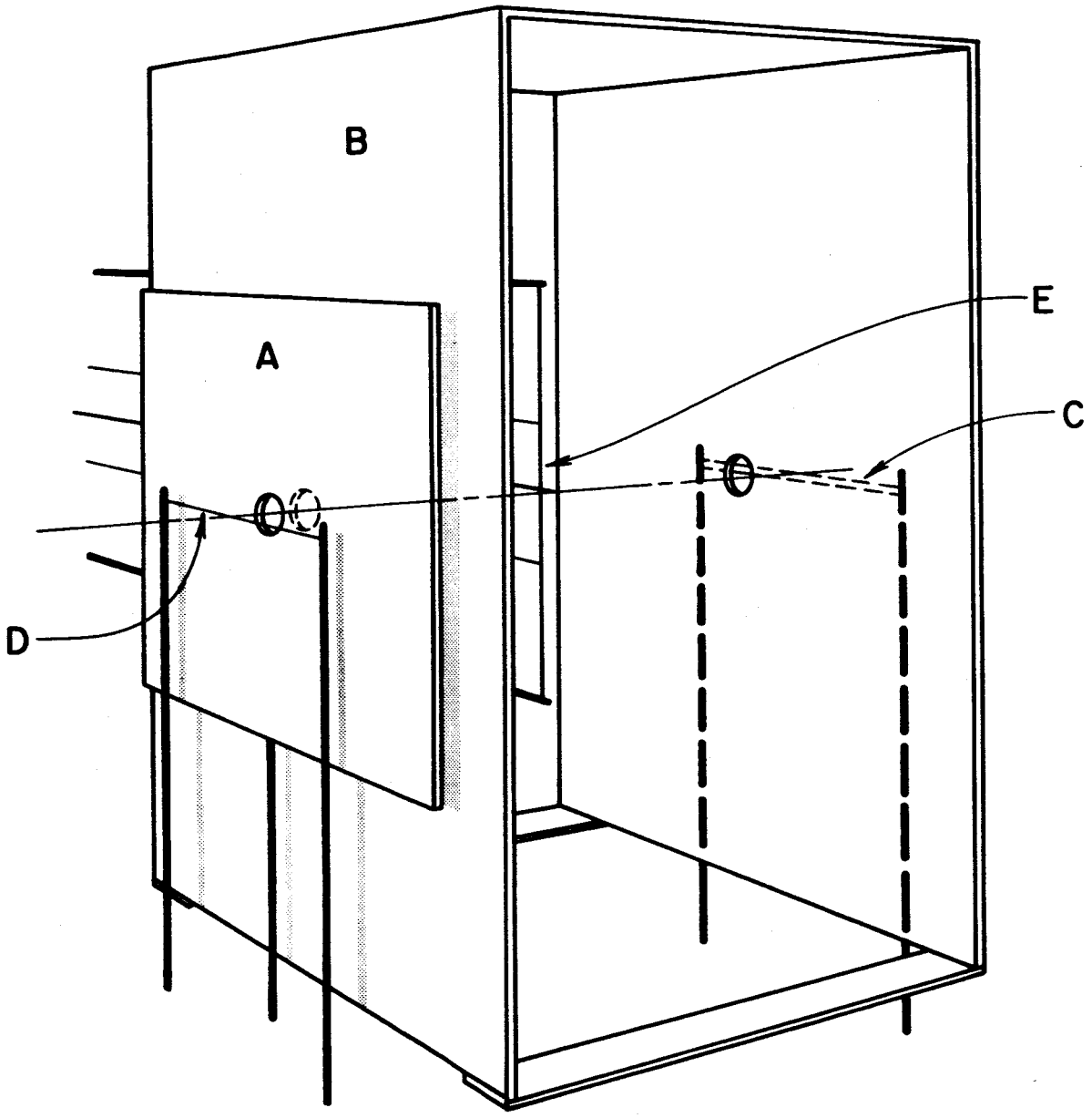

Figure 6. Diagram showing tip assembly, associated filaments and electrodes for quantitative study of emission heating and cooling.

field at the cathode tip, and ΔR is measured as a function of bombarding beam power at various cathode temperatures. Alignment of the electron beam so that it impinges on as small a section as possible of the 20 mil length field emitter is accomplished by first aligning the emitter structure so that only the very tip of the emitter protrudes through the 30 mil hole defined by the aperture on plate A, and then adjusting the direction of the magnetic field while simulataneously measuring the beam current striking the tip and the wire filament C in such a manner to insure that the electron beam is aligned with the defining apertures of plates A and B.

The actual power calibration (i.e., the resistance change per power exchange at the tip, hereafter referred to as c_o) of the emitter assembly was performed by measuring ΔR vs. the power input H at the emitter due to the bombardment current I_b at various emitter temperatures ranging from 300 to 1100°K; the slopes of such lines yielded the value of c_o(as shown in Figure 7) as a function of temperature. During the experimental measurements of ΔR vs. H the potentials of the various tube elements were as follows: V_D=222, V_A=0, V_B=200, V_e=0 and V_c=0 volts. This insures that the only secondary electrons able to reach the emitter are those originating from plate B; however, the error will be small since these electrons will possess nearly the full accelerating voltage. Furthermore, assuming perfect beam alignment, the number of secondary electrons formed at plate B should be negligible since the beam was determined to be sufficiently small to pass through the apertures.

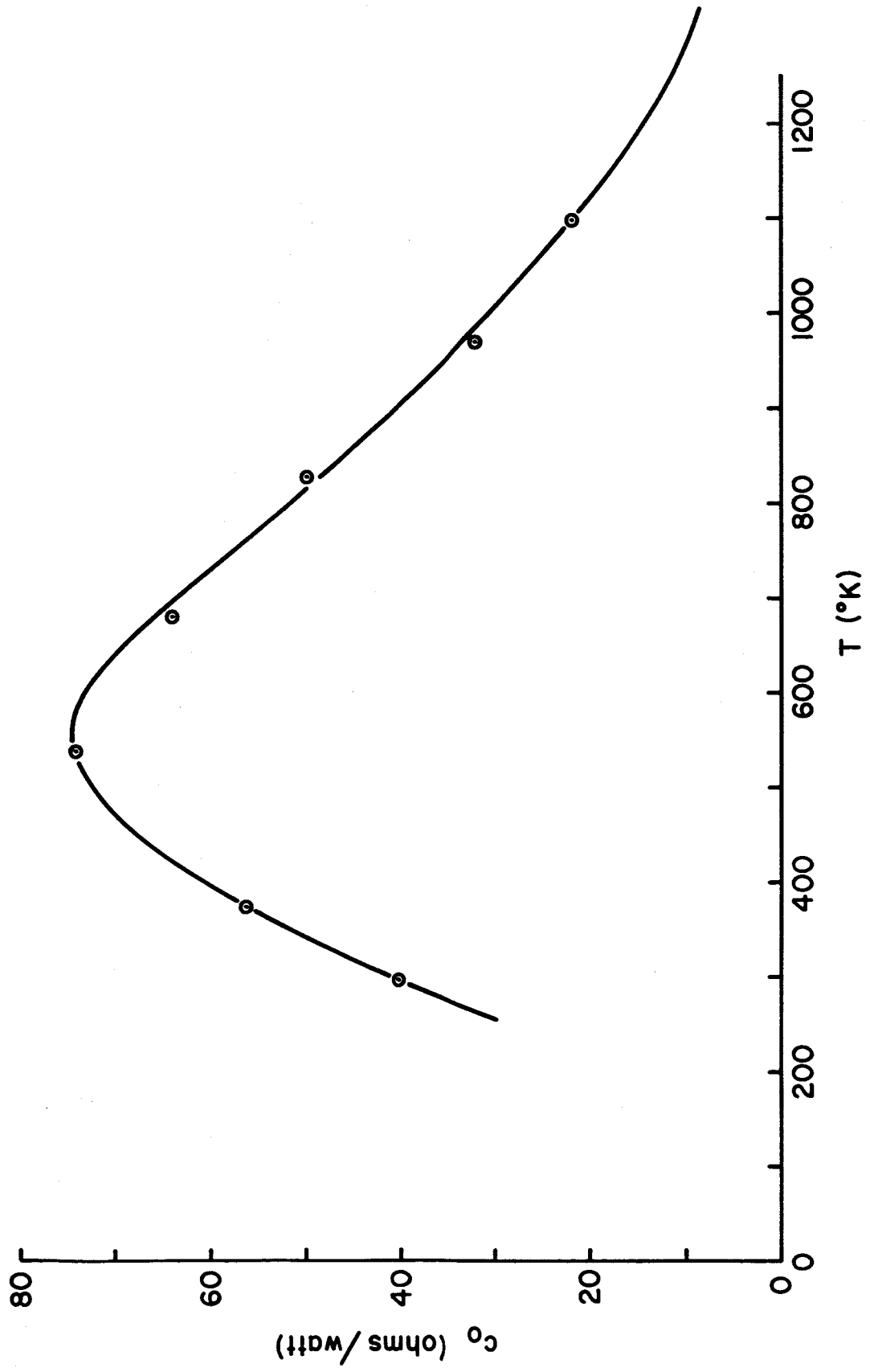

Figure 7. Plot of experimentally determined conversion factor (for converting ΔR changes to H) as a function of emitter temperature.

The collector filament C consisted of two 10-mil zirconium wires separated by 5 mil. This assembly served a two-fold purpose, namely; 1) to determine proper alignment and distribution of the bombarding beam during the emitter calibration, and 2) to serve as a source of zirconium for the purpose of changing the work function of the tip during the study of the Nottingham effect.

The tube envelope was made of alumino-silicote glass in order to eliminate helium pressure in the tube after seal-off. The tube embodiment was such that the field emission pattern from the emitter could be displayed on a fluorescent screen in order to ascertain the orientation and cleanliness of the emitter surface. Tip cleaning was accomplished by a combination of electron bombardment and resistive heating of the emitter. The vacuum was sufficiently low that negligible contamination of the emitter surface occurred for several hours after the initial cleaning. The β factor was obtained from the slopes m of Fowler-Nordheim plots which are related to β by the following equation:

$$\beta = \frac{2.83 \times 10^7 \phi^{3/2}}{m} \quad (cm^{-1}) \tag{14}$$

Thus, knowing the work function of the clean emitter, the average field can be evaluated from $F = \beta V$.

During the investigation of emission heating, field emission currents as high as 500 μa were drawn from the emitter. In order to minimize contamination of the tip, the magnetic field was applied such that the emitted current was collected on the plates B of Figure 6 which were tied

to anode potential, and which had previously been well outgassed by electron bombardment during the tube evaucation.

Voltage changes developed across the emitter support filament due to temperature changes at the tip, as caused by either emission heating or electron bombardment during calibration, were measured by a Keithley Model 660 differential voltmeter which was capable of measuring voltage changes with an accuracy of approximately 2 parts in 10,000. The current flowing through the emitter support filament was adjusted to the value necessary to give the required tip temperature (as determined by a previous calibration curve of filament resistance vs. temperature) and was also measured by the Keithley differential voltmeter by passing the filament current through a standard 1-ohm resistor and noting the voltage drop.

RESULTS AND DISCUSSIONS

Emission heating and cooling results were obtained on clean or nearly clean tungsten emitters and zirconium-oxygen coated tungsten emitters by drawing a certain field emission current and measuring the change in filament resistance ΔR, which could be converted to a power exchange H at the emitter from the conversion factors given in Figure 7. The upper limit of emitter temperature at which such measurements could be performed was determined by the onset of field-temperature induced rearrangement of the surface geometry, in the case of uncoated emitters, and rearrangement of adsorbed layers, in the case of zirconium-oxygen

coated emitters. Since the measured power exchanges range from 0 to 150 μw, it is important that the total power dissipated in the tube due to the field emission current be as small as possible in order to eliminate ambient temperature changes within the tube. In the case of clean tungsten, power dissipations as large as one watt were incurred due to the fact that the emitter was somewhat duller than expected and thus required larger voltages to obtain a given emission current. In order to minimize heating of the collector plates B of Figure 6, measurements of ΔR at a given I_e were taken as rapidly as possible. This problem was not as serious for the low work function surfaces where field emission voltages and, hence, maximum power dissipation required to draw a given I_e were reduced by the ratio of the work function change to the 3/2 power.

Another experimental problem capable of altering the emission heating results is the impingement of high energy ions on the emitter support structure which are formed at the anode. Such ions can be formed by electron induced desorption processes, since temperature changes were not sufficient to cause thermal desorption. Recent investigations of the latter phenomena[18-20] suggest that the number of ions formed per electron, particularly at voltages in excess of a few hundred volts, is less than 10^{-7} ions/electrons; thus, an electron current of 500 μa at 4 kv corresponds to an ion power input of 0.2 μw, which would be within the experimental error of the emission heating measurements. It is interesting to note, however, that ion currents as low as 10^{-13} amps can lead to rather high current densities at the field emission tip, even if one ion in 10^7 strikes the emitting

area. The latter was indeed observed in the case of zirconium-oxygen coated tungsten by a rapid decrease in the field emission current due to erosion of the adsorbed coating by impinging ions.

The results of power exchanges at the emitter as a function of emission current are given in Figures 8 through 12 for clean or nearly clean tungsten at various temperatures. It can readily be shown that the range of I_e and T over which experimental values of H were obtained is insufficient to cause appreciable resistive heating due to the emission current. For example, an approximate expression for the resistive power exchange H_r for an emitter of radius r and cone half-angle α is given by the following expression:

$$H_r = \rho_T \frac{I_e^2}{\pi \alpha r} \tag{15}$$

where ρ_T is the bulk resistivity at the desired temperature. For a typical emitter where $r=1.3\times10^{-5}$ cm and $\alpha=0.157$ radians, $H_r=1.4$ μw at $T=1000^{\circ}K$ and $I_e=600$ μa. Thus, the amount of resistive heating with a range of variables investigated is small and can be neglected.

Several observations can be made from the data given in Figures 8 through 12: First, it is noted that H increases with I_e in a near-linear fashion; second, it appears that the amount of heating at a given I_e decreases with temperature. Defining a symbol A as the energy per emitted electron exchanged with the lattice (positive A means energy given to the lattice), we can write the following expression:

$$H = I_e A = -\overline{\epsilon} I_e \tag{16}$$

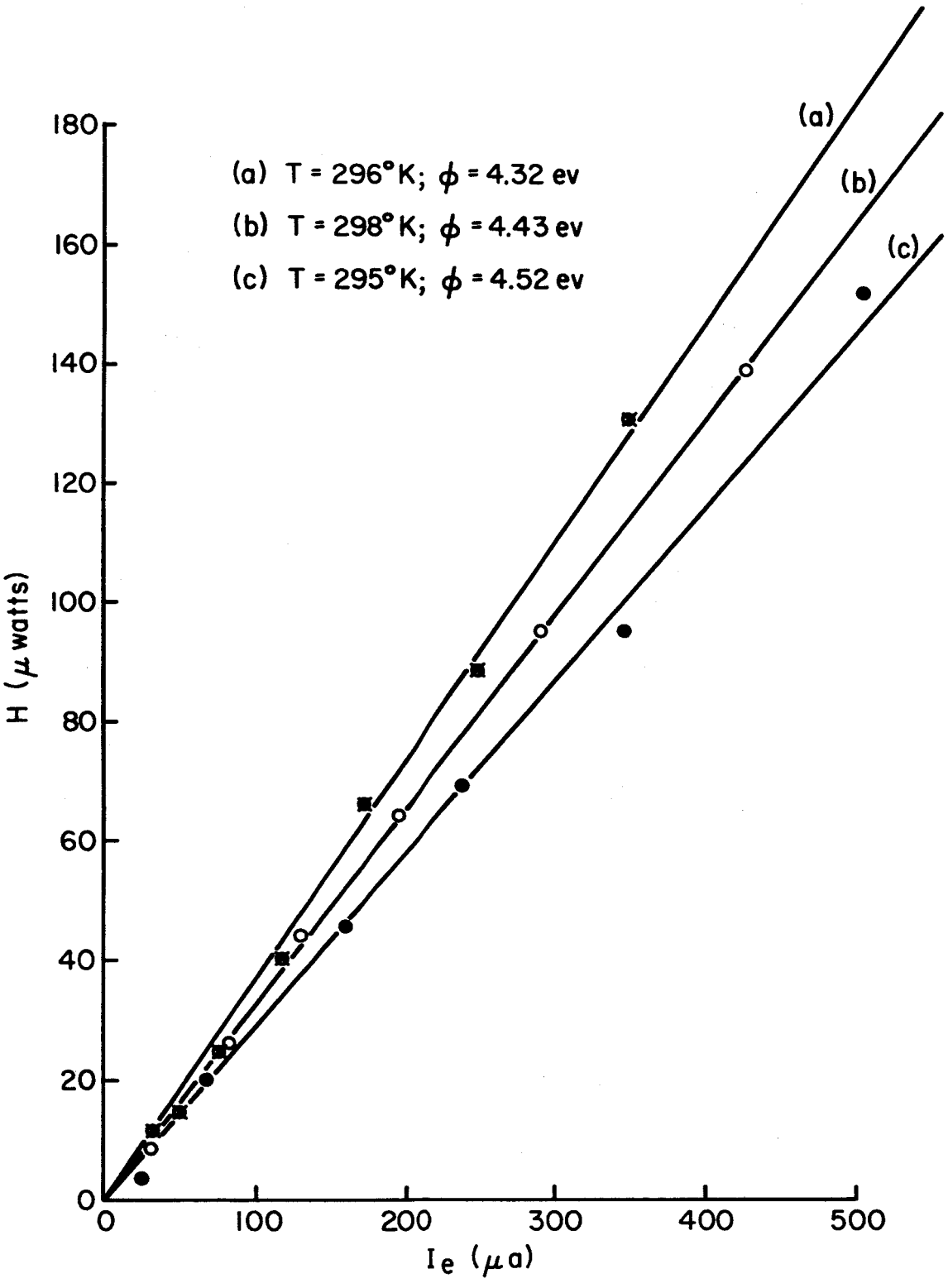

Figure 8. Experimentally determined power exchange H at the emitter as a function of field emitted current I_e at the indicated temperatures and work function.

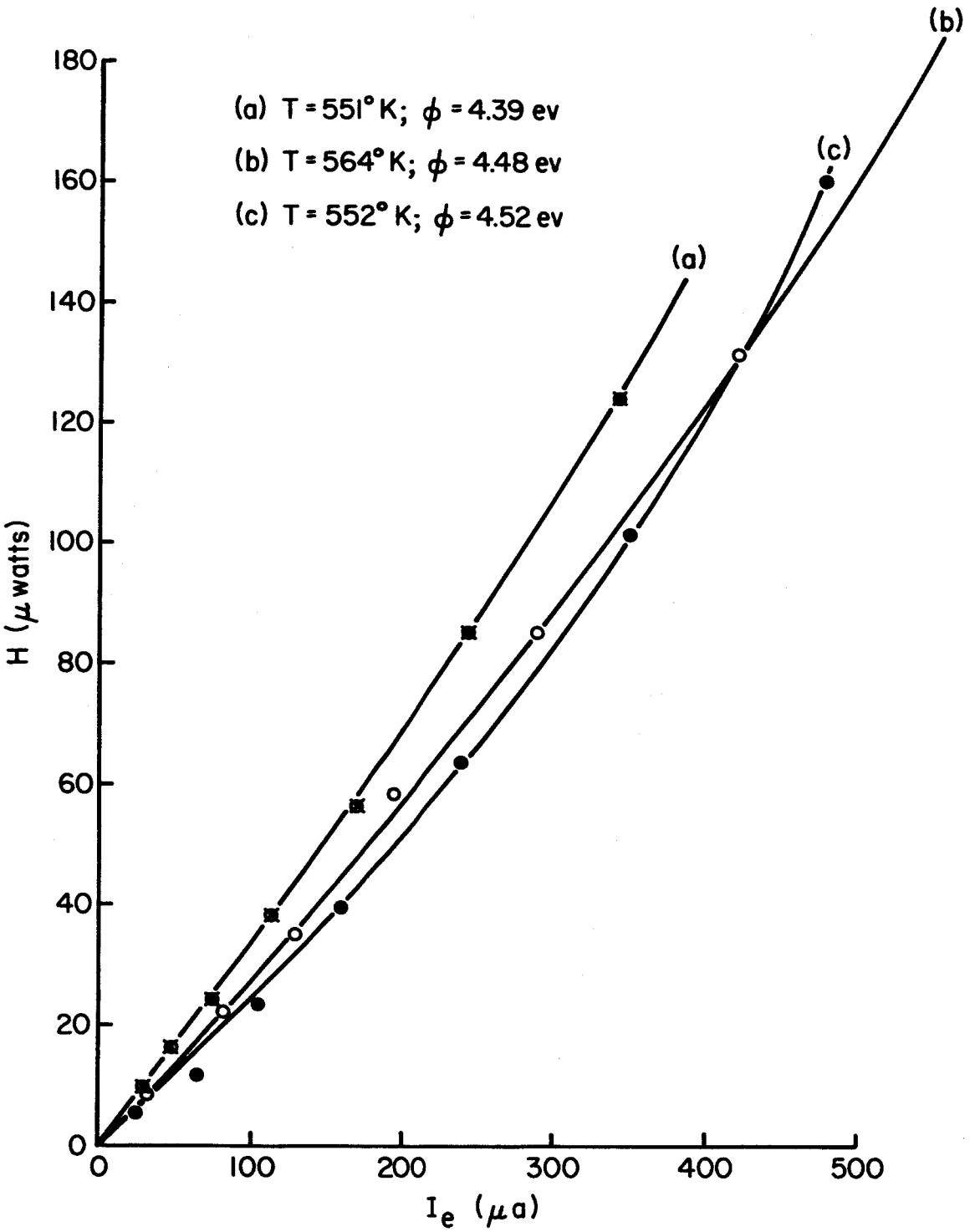

Figure 9. Experimentally determined power exchange H at the emitter as a function of field emitted current I_e at the indicated temperatures and work function.

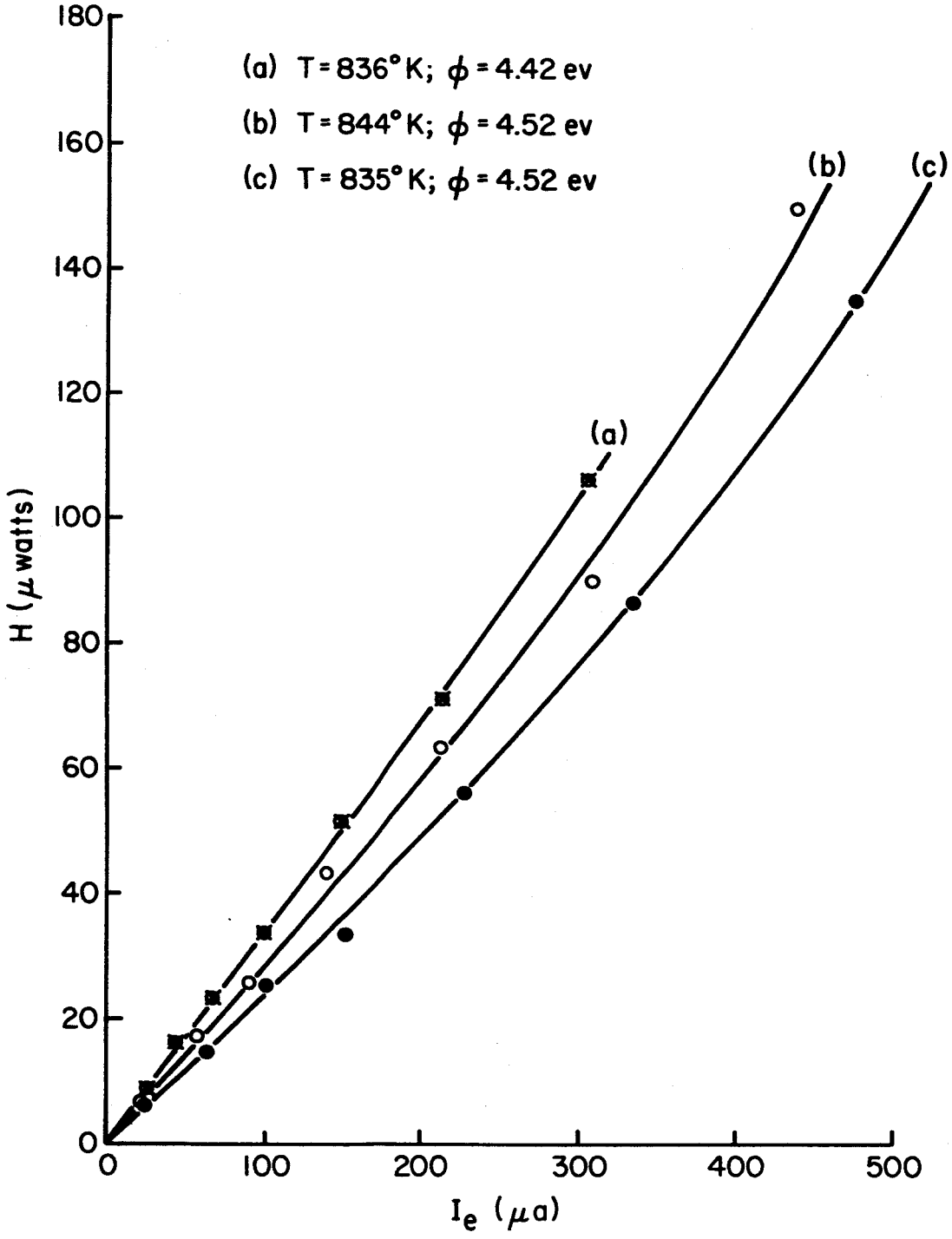

Figure 10. Experimentally determined power exchange H at the emitter as a function of field emitted current I_e at the indicated temperatures and work function.

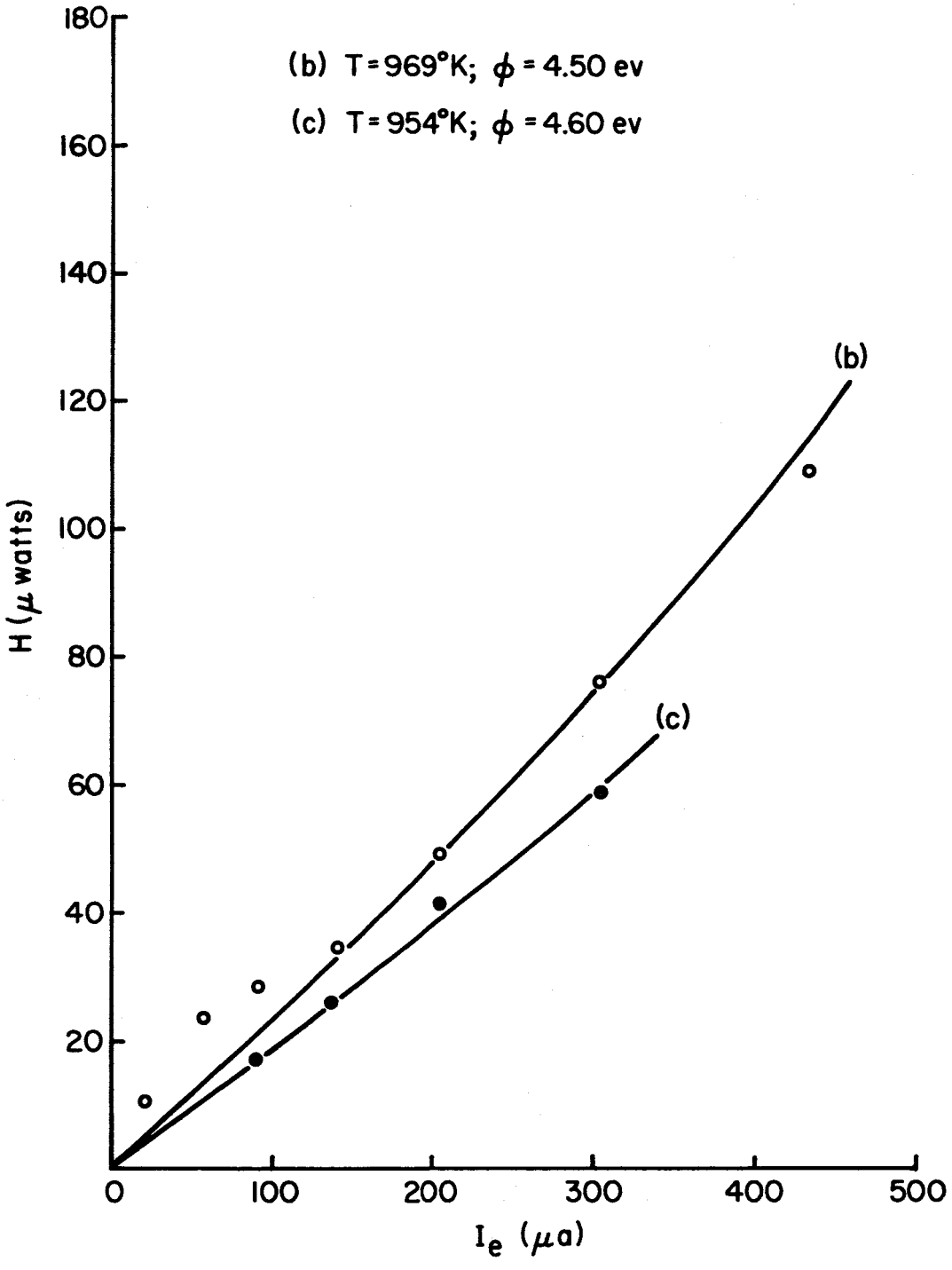

Figure 11. Experimentally determined power exchange H at the emitter as a function of field emitted current I_e at the indicated temperatures and work function.

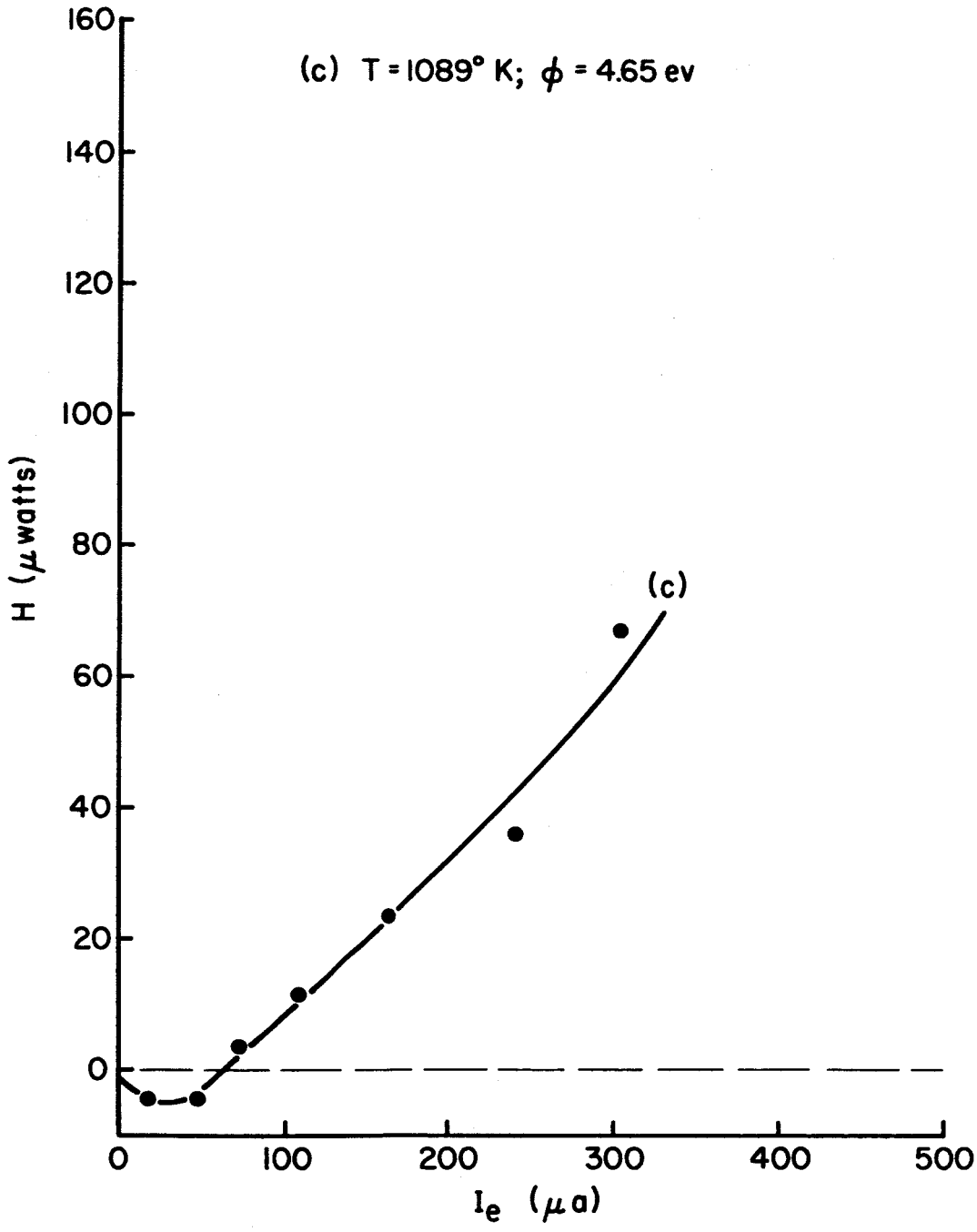

Figure 12. Experimentally determined power exchange H at the emitter as a function of field emitted current I_e at the indicated temperatures and work function.

If we further recall that the definition for the inversion temperature can be given as $p=T/2T^*$, then combining equations (12) and (16) one obtains the following:

$$H = I_e \pi k T \cot \frac{\pi T}{2T^*} \tag{17}$$

Hence, the two observed experimental trends, namely a near-linear increase of H with I_e and decrease with T are predicted by theory. It is further noticed that as T approaches T^* the variation of H with I_e will no longer be near-linear and depends more strongly on the variation of T^* with F and, hence, I_e. When the condition $T=T^*$ is reached, H=0; this is confirmed experimentally in results of Figure 12 which show an apparent transition from emission heating to cooling. Unfortunately, higher temperatures could not be investigated because of excessive rearrangement of the tip geometry at higher temperatures.

Similar results are given in Figure 13 for a tungsten emitter coated with zirconium-oxygen at various temperatures. Here it is observed that throughout most of the temperature range emission cooling occurs, i.e., $T > T^*$, and only at temperatures less than approximately 550°K does one observe emission heating. These results clearly show the crossing of the boundary which separates emission heating and cooling. Since the results at the various work functions are obtained over nearly identical regions of total field emission current, then according to equation (1) $\phi^{3/2}/F=c$, where c is a constant. Combining the latter condition with equation (13), one obtains the following equation:

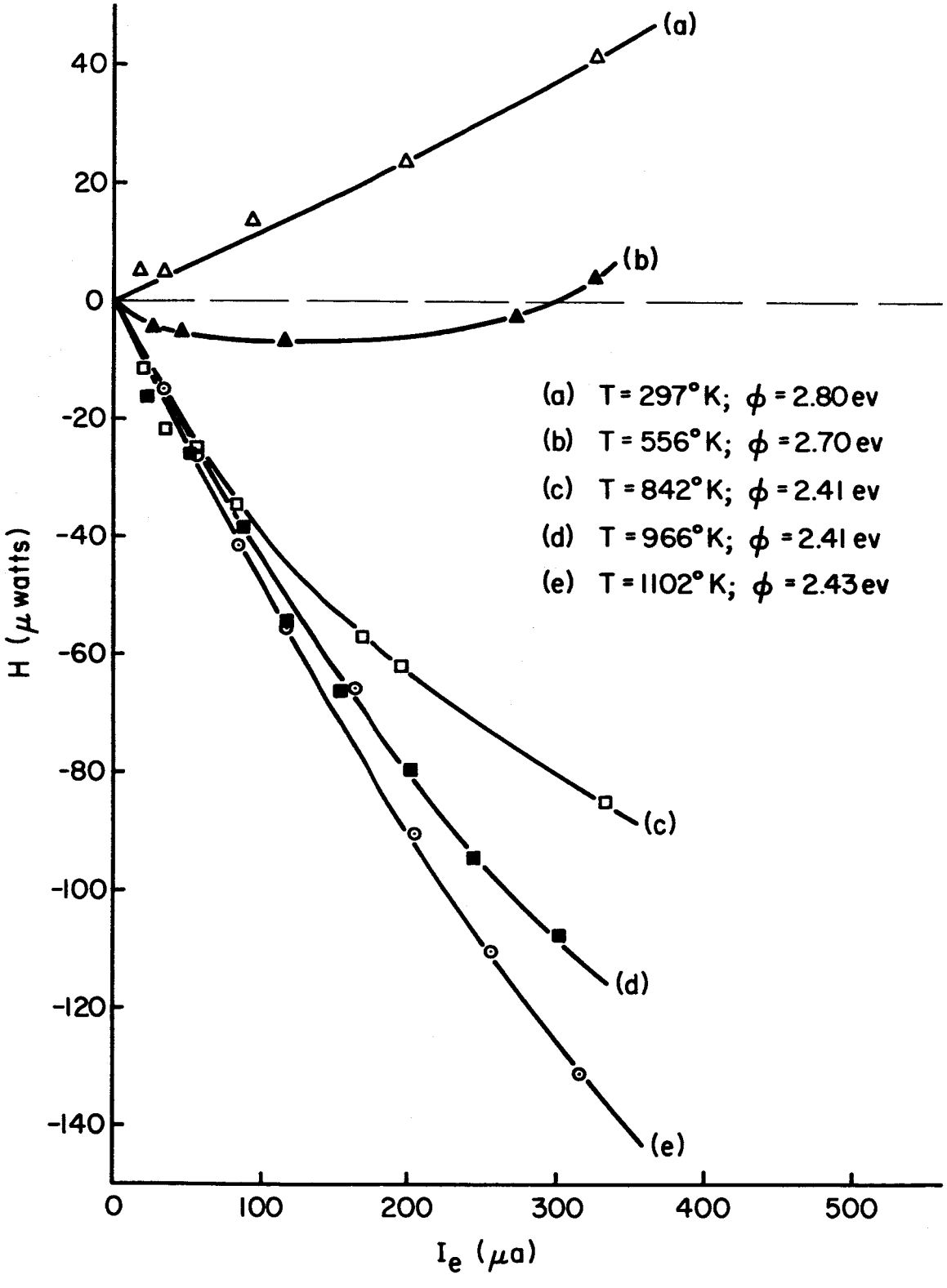

Figure 13. Experimentally determined power exchange H at a tungsten emitter coated with zirconium-oxygen as a function of field emission current I_e. Negative values of H indicate emission cooling.

$$T^* = \frac{5.67 \times 10^{-5} \phi}{t(y)\, c} \qquad (18)$$

which predicts a linear relationship between T^* and ϕ. One therefore would expect the observed decrease in T^* as the work function is diminished by the addition of adsorbed layers of zirconium-oxygen.

In order to make quantitative comparison of the experimental results with theory, smooth curves were drawn through the H vs. I_e data and values of $A = H/I_e$ were plotted against the value of applied field F as shown in Figures 14 through 18. Corresponding theoretical variations of the emission heating with field at the various temperatures and work functions are also given in Figures 14 through 18 for the purpose of comparison. Whereas the overall variations of the energy exchange per emitted electron with field, work function and temperature are in the direction predicted by theory, the discrepancy in the absolute value of the average energy exchange per emitted electron is large by a factor varying from 1.5 to 3. The variation between experiment and theory is largest for the 836°K results of Figure 16. It is interesting to note, however, that the theoretical and experimental curves converge and cross for the 1089°K results given in Figure 18. In view of the large percentage error associated with the amount of emission heating near the inversion temperature, the agreement between the experimental inversion field of 48.1 Mv/cm at 1089°K and the predicted value of 43.6 Mv/cm should be considered quite good.

The emission heating results given in Figure 19 for zirconium-oxygen coated tungsten show a wide variation of A from nearly 0.5 ev at

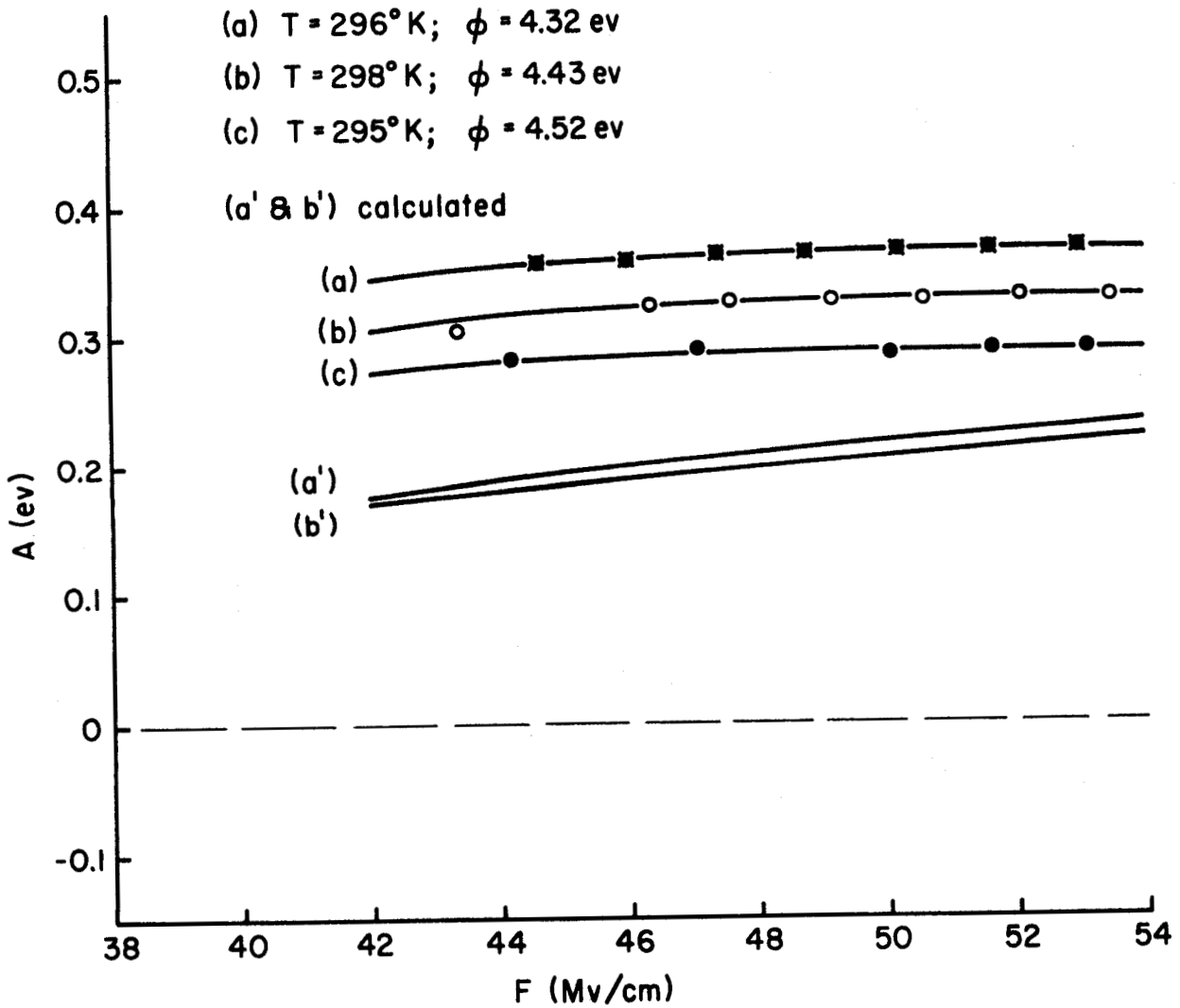

Figure 14. Experimentally determined energy exchange per electron A with the tungsten lattice as a function of applied electric field F at the indicated temperatures and work functions. Also shown are the corresponding theoretical curves calculated according to equation (12).

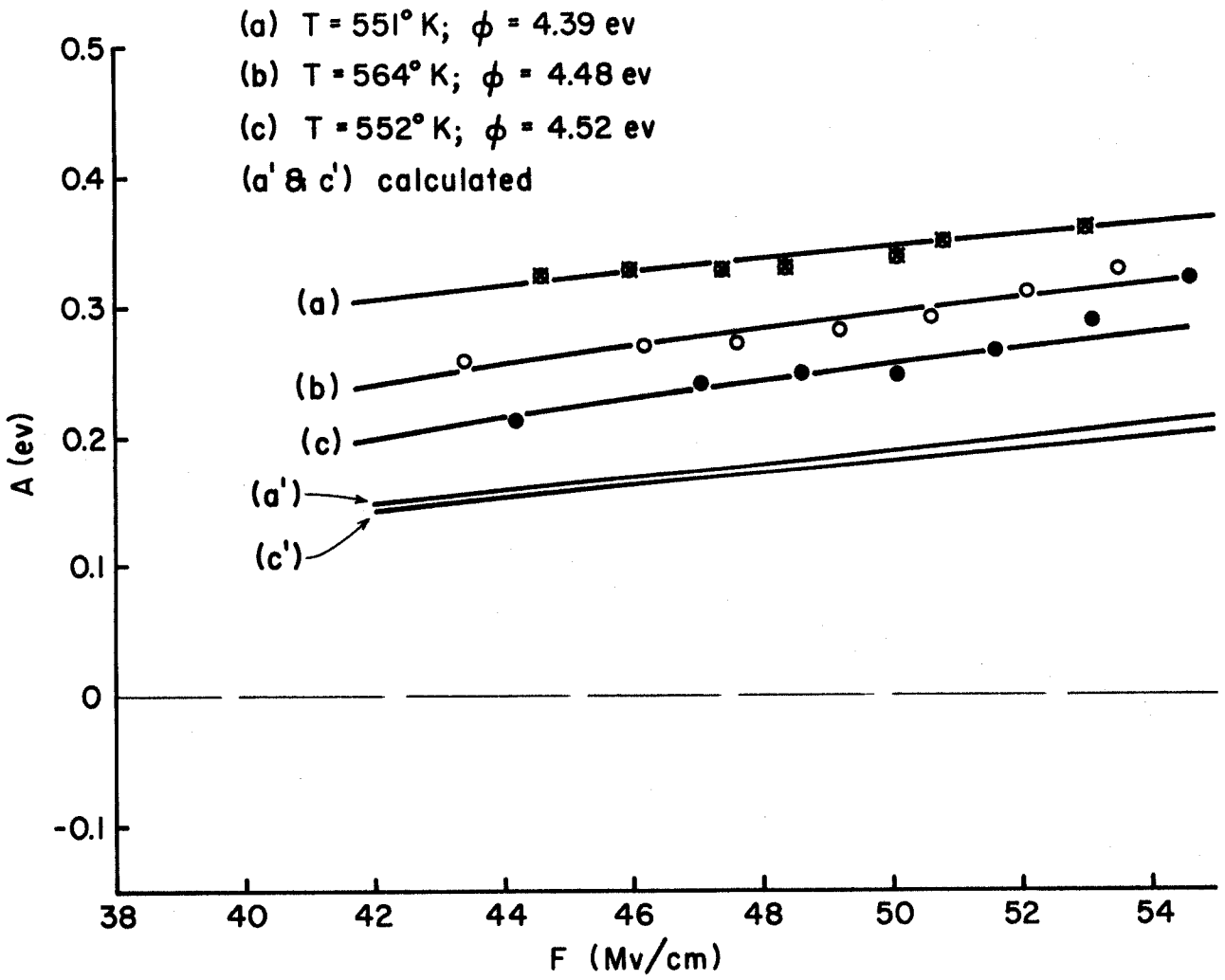

Figure 15. Experimentally determined energy exchange per electron A with the tungsten lattice as a function of applied electric field F at the indicated temperatures and work functions. Also shown are the corresponding theoretical curves calculated according to equation (12).

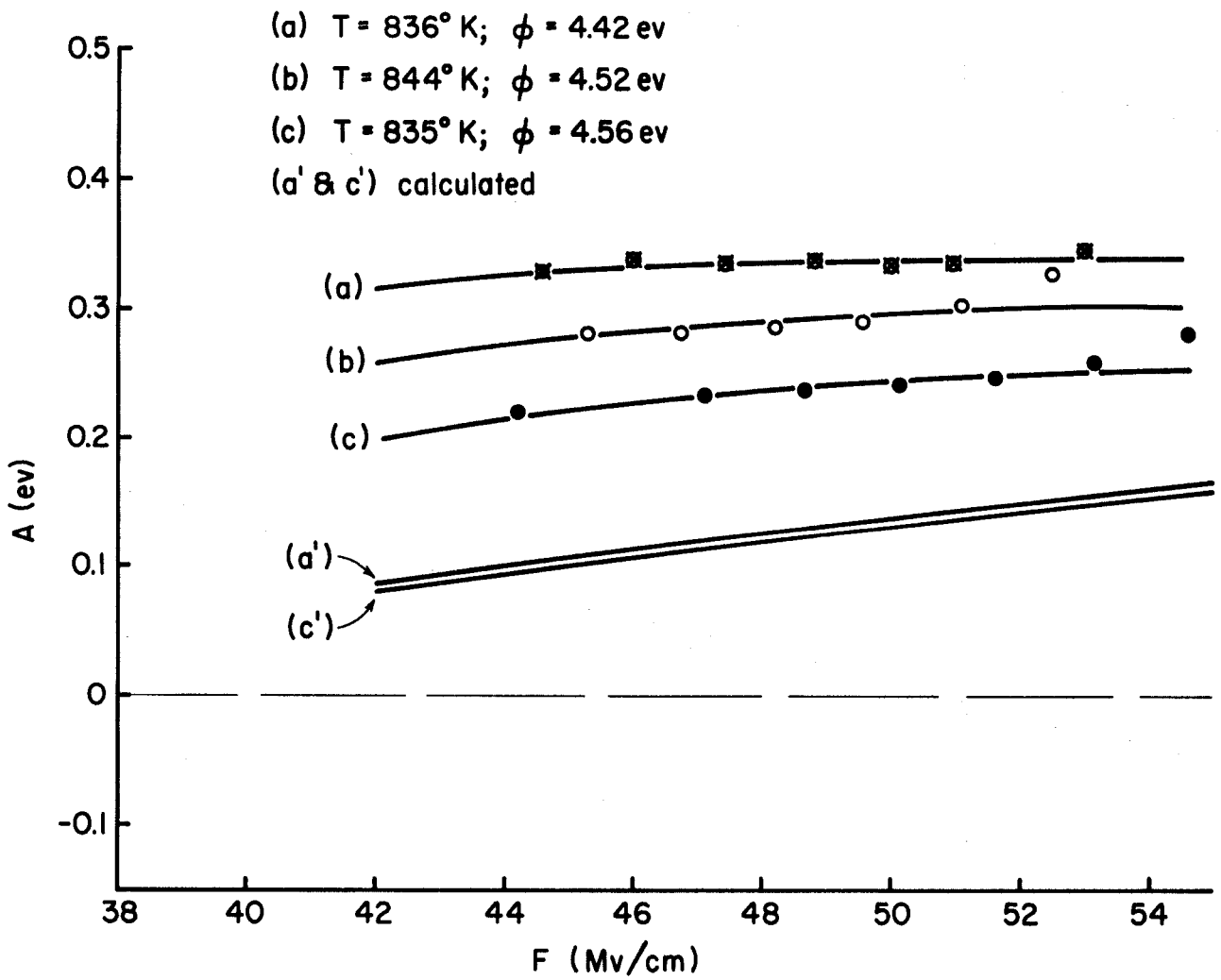

Figure 16. Experimentally determined energy exchange per electron A with the tungsten lattice as a function of applied electric field F at the indicated temperatures and work functions. Also shown are the corresponding theoretical curves calculated according to equation (12).

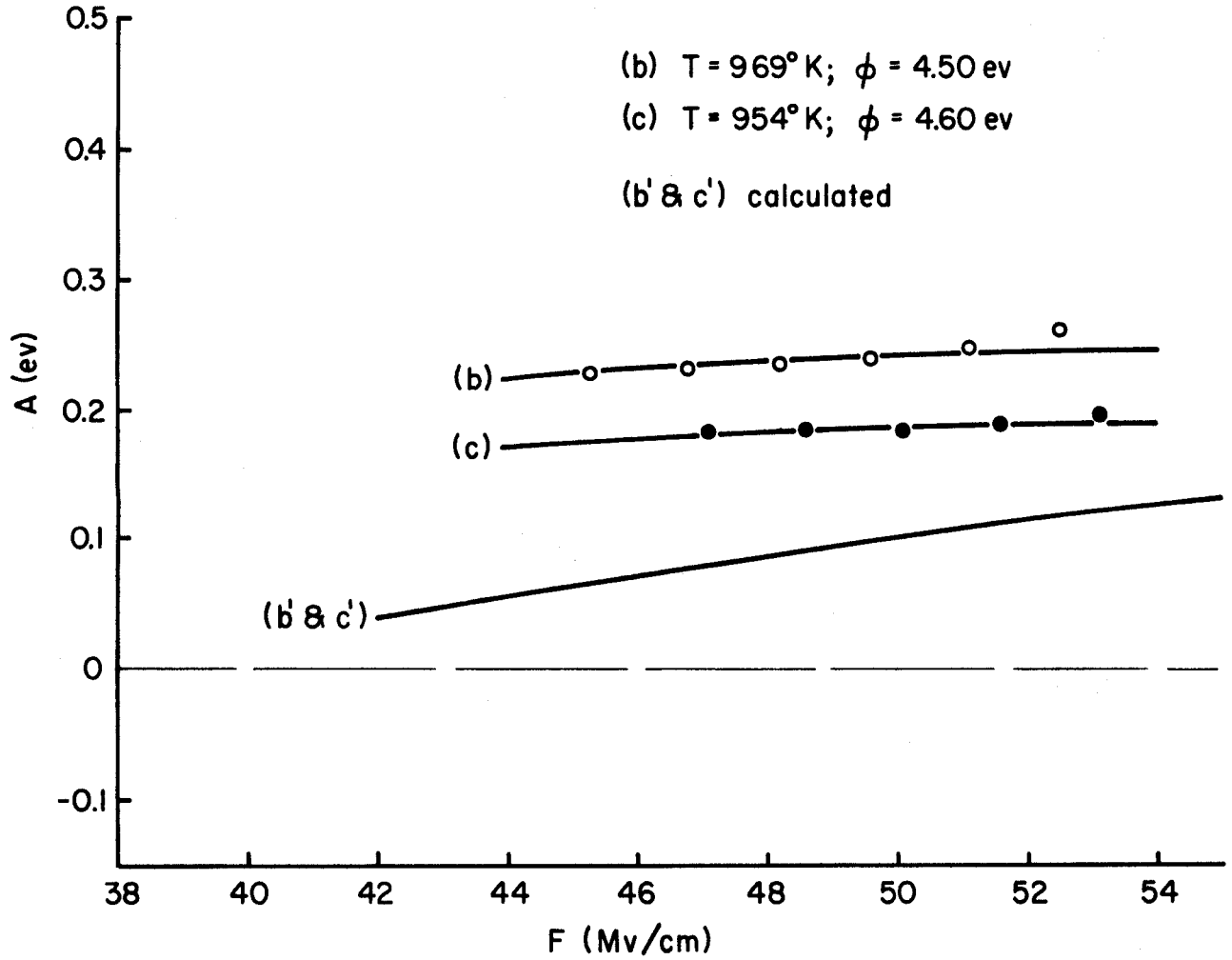

Figure 17. Experimentally determined energy exchange per electron A with the tungsten lattice as a function of applied electric field F at the indicated temperatures and work functions. Also shown are the corresponding theoretical curves calculated according to equation (12).

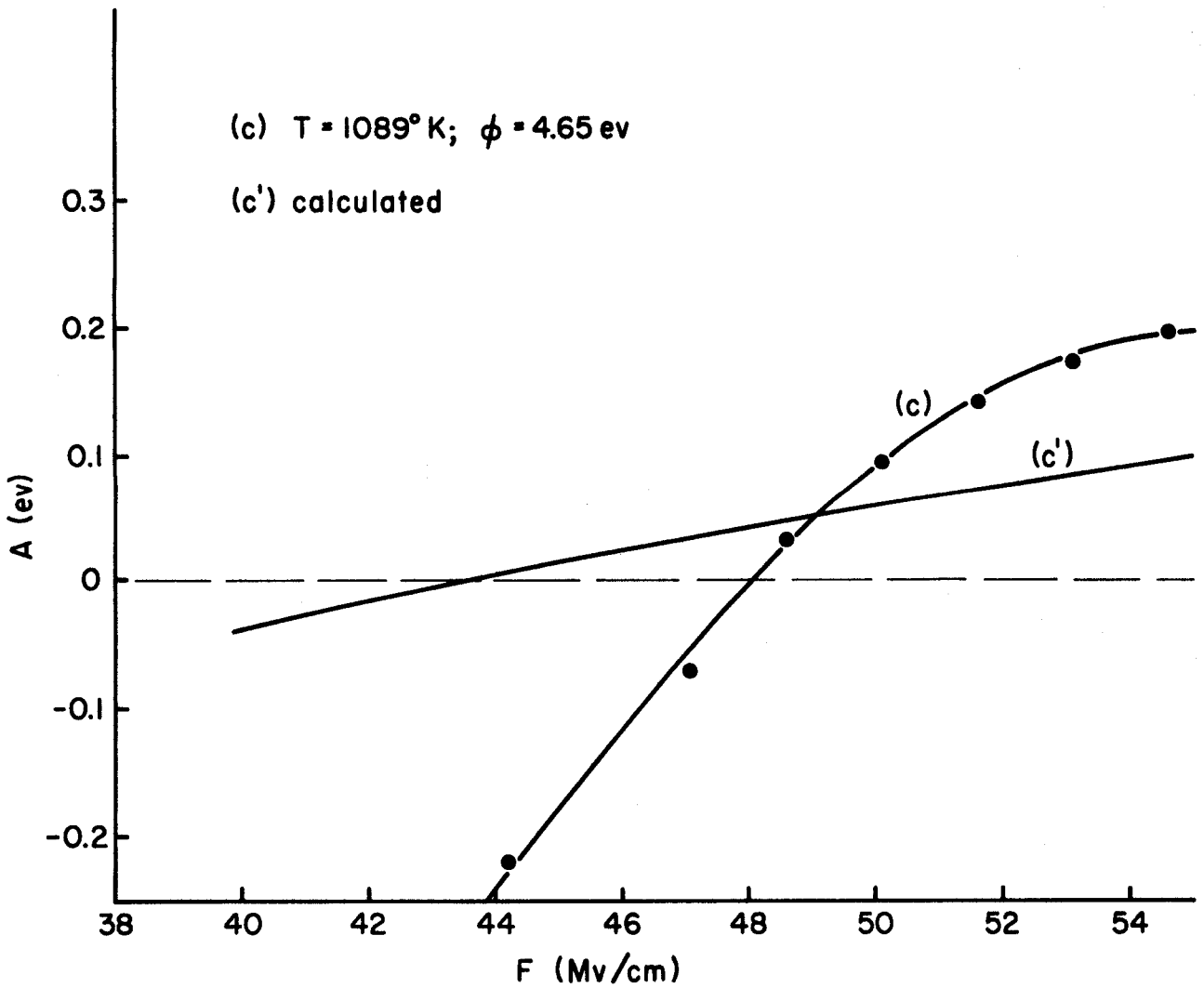

Figure 18. Experimentally determined energy exchange per electron A with the tungsten lattice as a function of applied electric field F at the indicated temperatures and work functions. Also shown are the corresponding theoretical curves calculated according to equation (12).

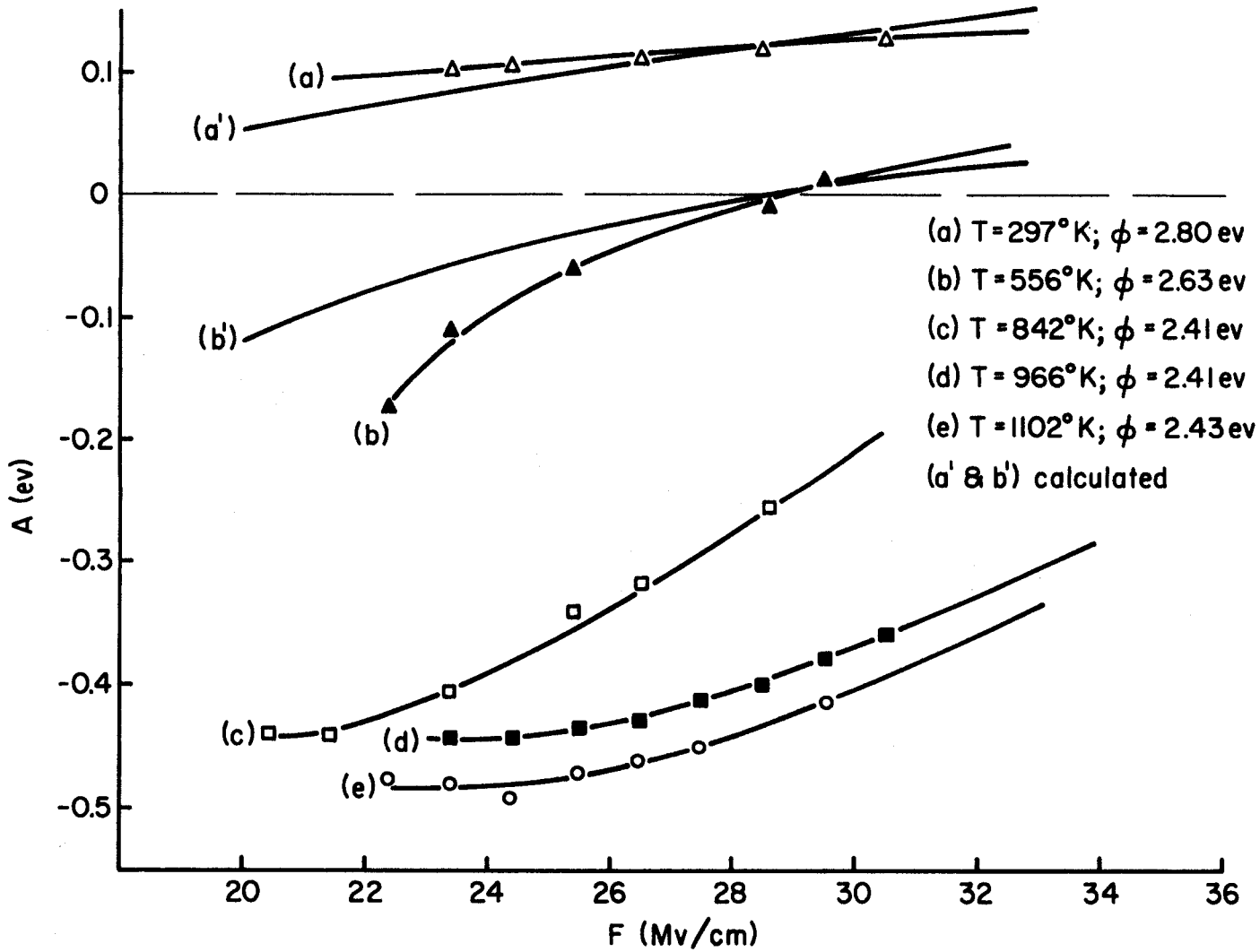

Figure 19. Experimentally determined energy exchange per electron A with the tungsten lattice as a function of applied electric field F at the indicated temperatures and work functions for a zirconium-oxygen coated emitter. Negative values of A indicate emission cooling. Calculated curves were determined according to equation (12) and assuming $p = 1.685\, p_{calc}$.

1102°K to 0.12 ev at 297°K. The striking feature of these results is the occurrence of the observed experimental inversion temperature at 556°K and a field of 28.8 Mv/cm which compares with a predicted value of T^*=938°K; thus, inversion temperature is lower than theory by nearly a factor of 2. Theoretical curves were plotted in Figure 19 for the 297 and 556°K results assuming $p=1.685\ p_{calc}$ which, in effect, caused the 556°K experimental and theoretical inversion fields to match. On this basis, the experimental and theoretical variations of A with F are reasonably close. No attempt was made to evaluate theoretical curves for the higher temperature results since the value of p suggested by the experimental results exceeds 2/3 and, therefore, T-F theory no longer applies.

In order to shed more light on the unexpected low values of T^*, the variation of T^* with F was measured over a limited range. These results, given in Figure 20 along with the expected theoretical variation, clearly show the discrepancy between experimental and theoretical values of T^*, but it is interesting to note that the variation of T^* with F appears to be linear as predicted by theory.

In order to gain further understanding of the reasons for these observed discrepancies between both the inversion temperatures for low work function surfaces and the absolute values of emission heating and cooling, further work will be necessary. It is expected that the energy distribution results will play an important role in elucidating some of the observed discrepancies. It should also be mentioned that the surprisingly low values for the inversion temperature have some practical implications for the utilization of zirconium-

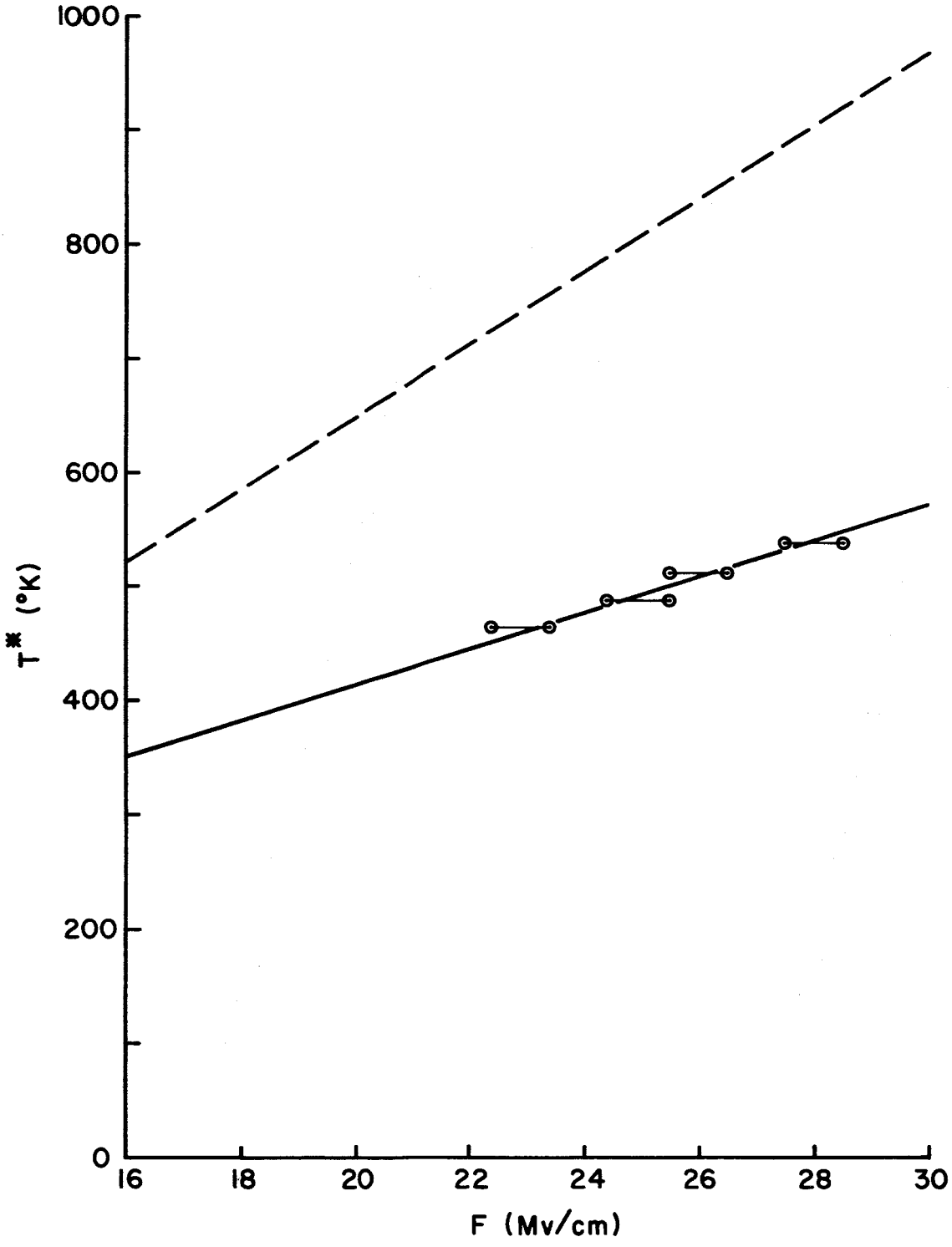

Figure 20. Experimentally determined inversion temperatures for a zirconium-oxygen coated tungsten emitter (ϕ = 2.67 ev) as a function of applied electric field. Dashed curve is calculated inversion temperature according to equation (13).

coated cathodes, particularly at high current densities. As mentioned in a previous section, emission cooling acts as a stabilizing effect on resistive heating effects which would be a regenerative process leading to vacuum arc in the absence of emission cooling. Both the large value of emission cooling at elevated temperatures and the low value of inversion temperature together tend to enhance this stabilizing effect. In further support of this, it has been observed experimentally that larger current densities are attainable from zirconium-oxygen coated tungsten electrodes than from clean tungsten.

SUMMARY

The emission heating results obtained thus far exhibit the proper trends expected by theory, but show certain discrepancies with regard to the absolute values of the emission heating and the inversion temperatures. Throughout the range of fields and temperatures investigated, with clean or nearly clean tungsten, the absolute value of emission heating appears considerably higher than predicted by theory; however, the value of the inversion temperature at a particular field agrees rather closely with theory. In the case of low work function surfaces, as obtained by depositing zirconium and oxygen on tungsten, the inversion temperatures observed are nearly a factor of 2 smaller than that expected by theory, although the general trends in the emission heating with temperature with field vary in the direction predicted by theory. On the basis of these results, one might expect the inversion temperature for a low work function surface as obtained by co-adsorption of cesium and oxygen on tungsten to be well below room temperature. Further

studies of this phenomena will be performed, utilizing barium as the adsorbate in order that emission heating and cooling may be investigated over a continuous range of work function from 4.5 to 2.1 ev.

TEMPERATURE DEPENDENCE OF WORK FUNCTION

In the case of refractory metal surfaces coated with alkali metal adsorbates, it has been observed[4] that the work function decreases with increasing temperature exhibiting a coefficient of approximately 10^{-4} ev/degree. Similar effects have been noted for zirconium-oxygen coated tungsten surfaces in the course of the emission heating experiments and will be discussed briefly.

The variation of work function with temperature can be evaluated from field emission techniques by two approaches, both utilizing the Fowler-Nordheim law of field emission given in equations (1), (2) and (10). The variation in slope of Fowler-Nordheim plots (I_e/V^2 vs. $1/V$) with temperature should be a measure of the variation of work function with temperature. More specifically, the ratio of the slopes m_1/m_2 of Fowler-Nordheim plots at two different temperatures, T_1 and T_2, can yield the ratio of the work function change according to the following equation:

$$\frac{\phi_1}{\phi_2} = \left(\frac{m_1}{m_2}\right)^{2/3} \tag{19}$$

thus, knowing ϕ_2 and the experimental values of the slope, one can calculate ϕ_1. It should be pointed out that the variation of work function with the

temperature obtained by the slope method must be used carefully, particularly at small F and/or large T since under these conditions p becomes large and the pre-exponential term $\pi p/\sin \pi p$ varies appreciably over the field range of experimental Fowler-Nordheim plots; the latter leads to a small curvature in the Fowler-Nordheim plots, which can be erroneously interpreted as a decrease in slope and, hence, work function. With these considerations in mind we have plotted in Figure 21 the change in work function (as determined from slopes of Fowler-Nordheim plot) relative to the room temperature value as a function of temperature. The curve of Figure 21 suggests a surprisingly strong decrease in the work function with temperature which is of the order of 10^{-3} ev/degree. More recent calculations have shown that part of the work function change, particularly at the high temperatures, may not be real due to curvature in the Fowler-Nordheim plots. This can be seen by comparing the Fowler-Nordheim plots obtained at room temperature and 110 1102°K as shown in Figure 22. Although the straight line portion of curve (b) gives a work function of 2.21 ev, the theoretical curve when plotted over several more orders of magnitude of current change indicates a curvature in the region we have assumed to be linear. Thus, if these corrections were made, the curve given in Figure 21 would undoubtedly show more flattening at the higher temperatures.

A fundamental reason for the work function change with temperature has not been clearly established at this time. Clean refractory metal surfaces also show a work function change; however, the coefficient is of the order of 10^{-5} to 10^{-6} ev/degree and is of opposite sign to the change

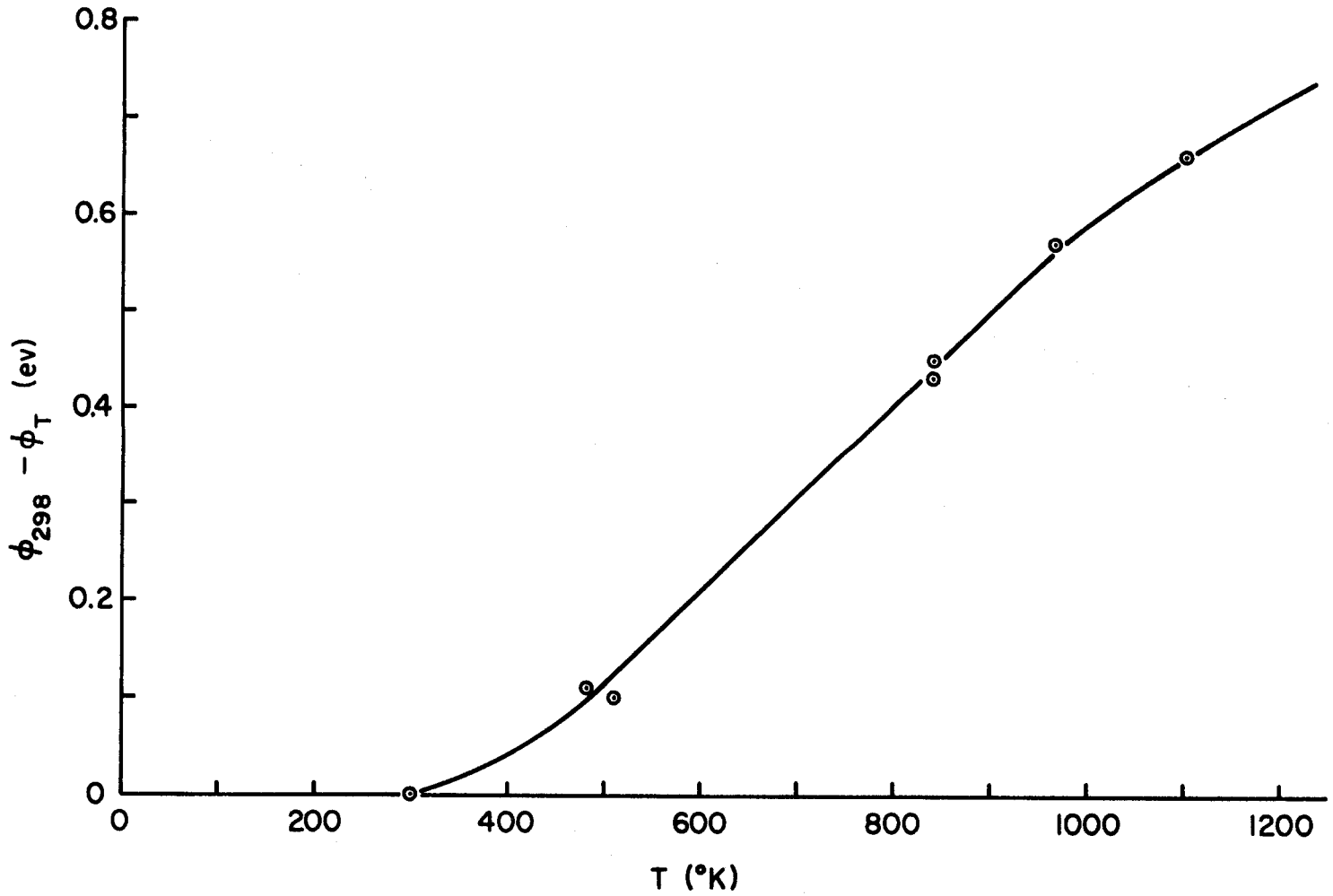

Figure 21. Plot of work function change of a xirconium-oxygen coated tungsten emitter (as determined from slopes of Fowler-Nordheim plots) as a function of emitter temperature.

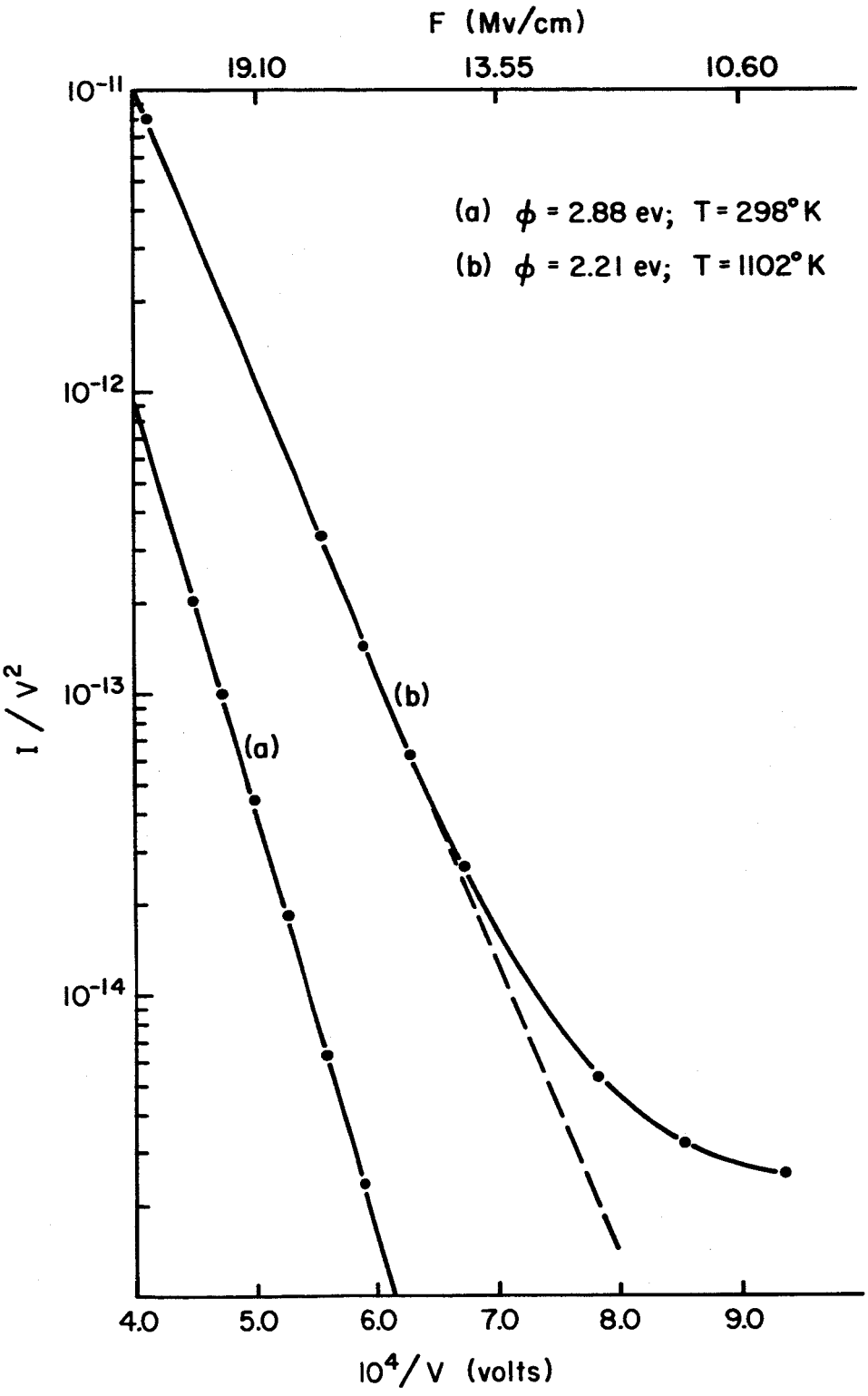

Figure 22. Fowler-Nordheim plots of a zirconium-oxygen coated tungsten emitter at two different values of emitter temperature. Curvature in curve (b) is due to increasing importance of T-F emission at high temperatures and low fields.

observed for adsorbed electro-positive layers. It has been speculated that the temperature dependence of work function of adsorbed layers is due to an increase in the effective dipole moment due to a rearrangement of the electronic distribution about the ad-atom as the latter is thermally excited into higher vibrational levels. Further experimental results of this nature for different substrate-adsorbate systems will be needed before a conclusive understanding of the mechanism can be obtained.

ENERGY DISTRIBUTION MEASUREMENTS

A tube is being constructed which will allow the measurement of the energy distribution of emitted electrons from various single crystallographic planes of the emitter and in the presence of certain adsorbed layers. Initially, we shall study the total energy distribution from clean tungsten as a function of temperature in order to determine the variation of the average energy of the emitted electrons. These results should have some bearing on the understanding of the emission heating results, since the latter suggest that the average energy of the emitted electron $-\bar{\epsilon}$ is larger than expected by existing theory. Similar correlations can be made between the emission heating and the total energy distribution results in the case of adsorbed layers and, in addition, certain parameters of practical interest such as beam noise and temperature can also be evaluated. The detailed construction of the energy distribution tube, its mode of operation, and preliminary results will be given in a forthcoming report.

FUTURE WORK

Besides the above-mentioned progress expected in the study of emission heating and energy distribution of the field emitted electrons, it is expected that further studies of the surface kinetics of co-adsorbed cesium and oxygen initiated under other support[4, 5] will be continued in the forthcoming quarter. In addition, a probe tube which provides capability of investigating adsorption pheomena and work function change on single crystallographic planes of a field emitter will be constructed and used in the cesium-oxygen co-adsorption studies.

REFERENCES

1. F. M. Charbonnier, R. W. Strayer, L. W. Swanson and E. E. Martin, Phys. Rev. Letters 13, 397 (1964).

2. F. M. Charbonnier, in Ninth Field Emission Symposium, Notre Dame University, June 1962 (unpublished).

3. E. E. Martin and F. M. Charbonnier, "Applied Research on Field Emission Cathodes", Final Report Contract No. DA36-039 AMC-03266(E), 1964.

4. L. W. Swanson, R. W. Strayer, C. J. Bennette and E. C. Cooper, "Behavior of Thin Alkali Metal Layers on Refractory Metal Substrates", Contract No. NAS 3-2596, 1964.

5. L. W. Swanson, R. W. Strayer, E. C. Cooper and F. M. Charbonnier, "Behavior of Thin Alkali Metal Layers on Refractory Metal Substrates", Contract No. NASw-458, 1963.

6. W. P. Dyke, J. K. Trolan, E. E. Martin and J. P. Barbour, Phys. Rev. 91, 1043 (1953).

7. W. W. Dolan, W. P. Dyke and J. K. Trolan, Phys. Rev. 91, 1054 (1953).

8. E. E. Martin, J. K. Trolan and W. P. Dyke, J. Appl. Phys. 31, 782 (1960).

9. O. A. Richardson, Phil. Trans. Roy. Soc. London, A201, 497 (1903).

10. W. B. Nottingham, Phys. Rev. 59, 907 (1941).

11. J. E. Henderson and G. M. Fleming, Phys. Rev. 48, 486 (1935); 54, 241 (1938); 58, 908 (1941).

12. Wright Air Development Division Technical Report No. 59-20 (AD-272760), January 1960 (unpublished).

13. F. M. Charbonnier, in Ninth Field Emission Symposium, Notre Dame University, June 1962 (unpublished).

14. P. H. Levine, J. Appl. Phys. 33, 582 (1962).

15. M. Drechsler, in Eighth Field Emission Symposium, Williams College, September 1961 (unpublished); Tenth Field Emission Symposium, Berea College, September 1963 (unpublished).

16. M. Drechsler, Z. Naturforsch. 18a, 1376 (1963).

17. R. D. Young, Phys. Rev. 113, 110 (1959).

18. D. Menzel and R. Gomer, J. Chem. Phys. 41, 3311 (1964).

19. D. Menzel and R. Gomer, J. Chem. Phys. 41, 3329 (1964).

20. P. A. Redhead, Can. J. Phys. 42, 886 (1964).